NASA TECHNICAL NOTE

NASA TN D-5774

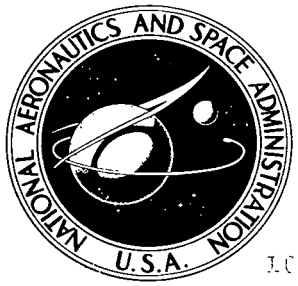

NASA TN D-5774

INSTABILITY OF SLENDER THIN-WALLED BOOMS DUE TO THERMALLY INDUCED BENDING MOMENTS

by Vernon K. Merrick

Ames Research Center
Moffett Field, Calif. 94035

NATIONAL AERONAUTICS AND SPACE ADMINISTRATION • WASHINGTON, D. C. • MAY 1970

1. Report No. NASA TN D-5774	2. Government Accession No.	3. Recipient's Catalog No.
4. Title and Subtitle INSTABILITY OF SLENDER THIN-WALLED BOOMS DUE TO THERMALLY INDUCED BENDING MOMENTS		5. Report Date May 1970 6. Performing Organization Code
7. Author(s) Vernon K. Merrick		8. Performing Organization Report No. A-3284
9. Performing Organization Name and Address NASA Ames Research Center Moffett Field, California 94035		10. Work Unit No. 125-19-03-04-00-21 11. Contract or Grant No.
12. Sponsoring Agency Name and Address NATIONAL AERONAUTICS AND SPACE ADMINISTRATION Washington, D. C., 20546		13. Type of Report and Period Covered TECHNICAL NOTE 14. Sponsoring Agency Code

15. Supplementary Notes

16. Abstract

The stability of slender thin-walled booms illuminated by thermal radiation is investigated. The problem is simplified by the assumptions that the cross section is thermally (but not necessarily structurally) seamless and thermal torques are negligible. This report is therefore a treatment of the influence of thermally induced bending moments on boom stability.

The linearized analysis developed shows that in the absence of structural damping, any initially straight boom, with either a seamless or open cross section, is unstable. The instability is an oscillatory divergence and is particularly severe for booms of open cross section. Stability can be attained by the use of flexural damping, but in many cases the amount required is greater than can be provided by the structure alone. Torsional damping is relatively ineffective.

A damper, in the form of a closed vessel, rigidly attached to the boom tip, and containing a ball free to move through a viscous fluid, is an effective stabilizer for a large class of booms important in space applications.

17. Key Words Suggested by Author Thermoelasticity Structural vibration Shells (structural forms) Gravity gradient satellites	18. Distribution Statement *Unclassified–Unlimited*

19. Security Classif. (of this report)	20. Security Classif. (of this page)	21. No. of Pages	22. Price*
Unclassified	Unclassified	63	$3.00

*For sale by the Clearinghouse for Federal Scientific and Technical Information
Springfield, Virginia 22151

TABLE OF CONTENTS

NOMENCLATURE

A	$\frac{L^3}{3EI} + \frac{L^5}{5R^2}\left[\frac{f_3(kL)}{4C} - \frac{1}{3EI}\right]$
a_n	coefficients of polynomial (n = 0, 1, 2, 3, 4, 5)
B	$\left[\frac{f_3(kL)}{2C} - \frac{1}{3EI}\right]\frac{L^5 \sin\alpha}{10RR_s}$
C	torsional rigidity
C_1	warping rigidity
c	thermal capacity
D	$\left[\frac{f_1(kL)}{2C} - \frac{1}{EI}\right]\frac{L^3}{3R}$
D_y, D_z, D_ψ	structural damping constants for damping of motions in y and z directions and in torsion about the boom axis
E	Young's modulus
EI	bending stiffness
e_c	coefficient of thermal expansion
F	$\frac{L}{C} f_2(kL)$
F_y, F_z	forces at tip of boom in $\bar{n}(L)$ and $\bar{b}(L)$ directions
$f_1(kL), f_2(kL)$ $f_3(kL), f_4(kL)$	functions defined by equations (B16), (B33), and (80)
G	$\frac{L^3 f_1(kL)}{6R_s C} \sin\alpha$
h	wall thickness
I	second moment of area of cross section
I_ψ	rotational inertia of tip mass
J_s	thermal radiation constant
K	thermal conductivity
k	$\sqrt{\frac{C}{C_1}}$

L	length of boom
M_t, M_n, M_b	moments about $\bar{t}$, $\bar{n}$, and $\bar{b}$ directions
$M_{y'}, M_{z'}$	bending moments about y_o' and z_o' axes
m_d	mass of the damper ball
m_d^*	$\frac{m_d}{m_T}$
$m_{d_m}^*$	minimum value of m_d^* for which the boom can be stabilized
m_s	mass of the damper case
m_T	total mass at the boom tip
$N(x,t)$	$R\int_0^x \eta(\hat{x},t)\sin\frac{x-\hat{x}}{R}\,d\hat{x}$
P	polynomial
p	real part of unstable root
p^*	dimensionless p, $p\sqrt{m_T(A-B)}$
q	imaginary part of unstable root
q^*	dimensionless q, $q\sqrt{m_T(A-B)}$
R	total radius of curvature
R_o	initial radius of curvature
R_s	thermally induced radius of curvature
r	radius of boom cross section
s	Laplace transform variable
s	distance measured along the circumference of the boom cross section (used only in appendix A)
s^*	dimensionless Laplace transform variable, $s\sqrt{m_T(A-B)}$
T	couple at tip of boom in $\bar{t}(L)$ direction
T	perturbation temperature $(\bar{T} - T_o)$ (used only in appendix A)
$\bar{T}$	absolute temperature of a point on the boom

T_o	mean absolute temperature of boom
t	time measured from the instant the boom is perturbed from its thermal equilibrium position
t'	time measured from the instant the boom received radiant heat
$\bar{t}(x),\bar{n}(x),\bar{b}(x)$	tangent, normal, and binormal unit vectors defined at a point x along the boom axis
U_B	strain energy in bending
X	relative stiffness parameter, $\frac{B}{A}$
x,y,z	distances measured along the boom axis and along $\bar{b}(x)$ and $\bar{n}(x)$, respectively
x_o,y_o,z_o	rotated coordinate system: the $x_oy_oz_o$ system is derived from the $x_o'y_o'z_o'$ system by a positive rotation α about the x_o' axis; the boom in equilibrium lies in the x_oy_o plane
x_o',y_o',z_o'	basic coordinate system: x_o' is measured along the tangent at the boom root, positive in the direction of the tip, y_o' is perpendicular to x_o' and such that the sunline is in the $x_o'y_o'$ plane, z_o' completes the orthogonal right handed system
y',z'	axes parallel to y_o' and z_o' at a typical point on the boom axis
y'',z''	axes rotated through angle ψ relative to y', z' axes (boom fixed axes)
α	angle between the normal to the plane of bending in the equilibrium state and the y_o' axis (see fig. 1)
α_s	absorptivity
β	angle between radiation rays and y_o' axis (sunline lies in the $x_o'y_o'$ plane)
γ	input heat flux rate due to thermal radiation
Δ	small change in a variable
δ	angle between the normal to the plane of initial bending and the y_o' axis (see fig. 1)
ε	emissivity

ζ_z flexural damping factor, $\frac{D_z}{2m_T}\sqrt{m_T(A - B)}$

$\zeta_{z'}$ flexural damping factor, $\frac{D_z}{2m_T}\sqrt{\frac{m_T L^3}{3EI}}$

ζ_ψ torsional damping factor, $\frac{D_\psi L f_2(kL)}{2C}\sqrt{\frac{3EI}{m_T L^3}}$

$\eta(x,t)$ $\frac{\Delta M_{y'}(x,t)}{M_{z'}(\infty)}$

κ damping constant of ball damper

κ^* dimensionless κ, $\frac{\kappa\sqrt{m_T(A - B)}}{m_d}$

λ reciprocal of the principal thermal time constant

λ_n reciprocals of time constants of thermal modes ($n = 0, 1, 2, \ldots$)

λ^* dimensionless λ, $\lambda\sqrt{m_T(A - B)}$

ν Poisson's ratio

ρ mass density of the boom material

ρ_ψ radius of gyration of tip mass, $\sqrt{\frac{I_\psi}{m_T}}$

σ Stephan-Boltzmann constant

σ_I rotational inertia of boom per unit length

σ_m mass per unit length of the boom

ψ angle of twist relative to the boom root

$(\ )_o$ variable associated with an initially straight boom

INSTABILITY OF SLENDER THIN-WALLED BOOMS DUE TO THERMALLY INDUCED BENDING MOMENTS

By Vernon K. Merrick

Ames Research Center

SUMMARY

A linearized dynamic stability analysis of slender booms illuminated by thermal radiation is developed. It is assumed that the booms have thin-walled, circular cross sections. In addition the cross sections are assumed to be thermally (but not necessarily structurally) seamless and thermal torques about the boom axis are assumed to be negligible. The analysis is therefore concerned with the influence of thermal bending moments on boom stability.

It is shown that in the absence of structural damping, any initially straight boom, with either a seamless or structurally open cross section, is unstable. Booms with an initial curvature may exhibit either oscillatory or nonoscillatory instabilities, depending on the magnitude and direction of the initial curvature. The worst case oscillatory instability has a frequency 66 percent of that of the natural flexural frequency and diverges as if it had a damping factor of -0.354. The instability can be suppressed by flexural damping but, in general, the amount required is greater than can be provided by the structure of existing boom types. Torsional damping is relatively ineffective and there exists a class of booms which cannot be stabilized by torsional damping.

Initial boom curvature can have a significant effect. If the initial curvature is such that the boom, in the equilibrium state, is bent toward the radiation source, it is stable; otherwise it is unstable. In general, the stability of a boom is only slightly influenced by whether or not the boom cross section is restrained from warping at the tip.

A damper, in the form of a closed vessel, rigidly attached to the boom tip and containing a ball free to move through a viscous fluid is an effective stabilizer for a large class of booms important in space applications.

INTRODUCTION

Consider an idealized situation in which a slender, thin-walled boom, clamped rigidly at one end, is placed in a force-free environment. Suppose this boom is suddenly illuminated by uniform planar radiation such as, for example, solar radiation. Some of the radiant energy will be absorbed by the boom and will set up internal thermal gradients. These, in turn, will produce

internal stresses causing the boom to bend and twist. In the process of bending and twisting, elements of the boom will change their orientation relative to the direction of the incident radiation. Thus, the thermal stresses and, therefore, the effective thermally induced bending moments and torques will change as the boom deforms. In concept, at least, the boom will ultimately adopt some static equilibrium shape. The calculation of static equilibrium shapes for booms of open cross section is treated thoroughly in reference 1. However, neither static nor dynamic stability of the boom is considered. There is, therefore, no guarantee that all or even any of these static equilibrium shapes will occur in practice.

The first indication that all static equilibrium shapes are not stable was both sudden and dramatic. The OGO IV satellite which has a 60-foot-long boom of open cross section began to exhibit high frequency attitude oscillations whenever it was exposed to sunlight. It was found by the Stabilization and Control Branch at Goddard Space Flight Center that this behavior could be explained if it was assumed that the boom was oscillating at its fundamental bending frequency with an amplitude at the tip of about 14 feet. This information became available at a time when many gravity stabilized satellites were exhibiting apparently random anomalous attitude behavior. Since long booms of open cross section are common features of these satellites, it was conjectured that boom instability could be the source of the difficulties. High frequency oscillations recently observed in the magnetometer readings of one of these satellites tend to support this conjecture. The final evidence supporting the possibility of boom instability was provided by the Structural Dynamics Branch at Ames Research Center where thermal oscillations were produced in a relatively short boom. This demonstration provided incontrovertible proof of the possibility of thermally induced dynamic instability in booms of open cross section.

In retrospect, a hint that the stability of booms may be a significant question is given in reference 1, which points out, clearly, that the bending and twisting modes are coupled. The existence of coupled structural modes together with bending moments and torques that are functions of structural deformation are classical elements in the production of instabilities. Numerous examples can be found in the field of aeroelasticity.

There are several approaches to the theoretical study of thermally induced boom instabilities. An extension of the comprehensive approach of reference 1 to include dynamic effects should produce details of the actual boom motions that will be encountered. An important contribution along these lines has been given by Frisch in reference 2. However, with this type of approach it is often difficult to assess the relative importance of the various boom system parameters. Therefore, in addition to a precise analysis, there is a need for a more traditional engineering approach in which the model of the phenomenon is drastically simplified to the point where only the most important factors are retained. With such a theory there is hope of obtaining insight into the basic causes of boom instability and into possible means of preventing it. Analysis of possible thermal instability mechanisms have already been made by Yu (ref. 3) and Beam (ref. 4). The mechanisms in both cases were relatively simple although they differed widely in concept. Yu analyzed a situation in which changes in thermal bending moments, due solely to boom flexure, provide

the mechanism for converting heat energy to mechanical energy. The type of boom cross section in this case is not important. One result of this theory is that the greatest instabilities occur when the axis of the boom lies along the direction of the radiation. In contrast, Beam presents an analysis, supported by experiment, of the influence of thermal torques on stability. An essential feature of the type of boom treated is that it has an open nonoverlapping cross section. The greatest influence of thermal torques must, of course, occur when the boom axis is perpendicular to the direction of radiation. Beam discovered that booms could exhibit both instability and improved damping, depending on the orientation of the boom split relative to the direction of radiation.

The purpose of this report is to analyze yet another mechanism for the production of thermal instability. Consider a boom which, in its unheated state, has its axis normal to the direction of radiation. The static equilibrium shape will generally be such that the boom is bent away from the radiation source. A bent boom has the well-known structural property of coupled flexure and torsion. Thus a force applied to the end of the boom in a direction perpendicular to the plane containing the boom axis will produce not only bending but also twisting. This effect is particularly marked for a boom of low torsional rigidity. The boom twist produced by the force causes thermal bending moments that tend to restore the plane of bending back to its original direction. The analysis presented here seeks to determine how boom stability is influenced by bending moments due to twist. It is clear that the basic physical mechanism described above has many similarities to that underlying the in-flight dynamic behavior of an airplane wing. Once this analogy is recognized it becomes easier to understand how a thermally bent boom can exhibit instabilities. Since in a practical boom system employing an open cross section thermal torques and thermal bending moments due to twist must coexist, the analysis of this report may be regarded as complementary to that of Beam in that any general theory of boom stability must contain essential elements from both theories.

The analytical approach adopted here is based on the linearized analysis of what is probably the simplest conceivable boom system. One major simplifying characteristic of this system is derived from the assumption that the cross section provides a continuous conduction heat path. The cross section is therefore thermally seamless (although not necessarily structurally seamless), which greatly simplifies the calculation of the thermal bending moments. A second major simplifying characteristic is derived from the assumption that the effective mass of the boom may be considered to be located at the free end. This assumption ensures the existence of a single mode of bending and a single mode of twist. A third major simplification is that thermal torques are negligible. This assumption is strictly true only if the cross section is structurally seamless. This boom system is not particularly representative of the open overlapped cross section booms used in space applications. On the other hand, the behavior of the idealized boom system can provide basic information relevant to an understanding of the observed behavior of actual boom systems. In particular, the analysis provides an immediate answer to the basic question of whether or not thermal bending moment instabilities are possible with a boom having a structurally seamless cross section.

The analysis is extended beyond that which would be required to analyze the stability of a simple, initially straight boom. The influence of small amounts of initial boom curvature (such as might be introduced during manufacture) is investigated, along with the possibility or providing stability by means of a simple, passive, ball damper located at the tip of the boom.

DERIVATION OF THE STABILITY POLYNOMIAL

Four steps are required to develop the stability polynomial. The first step is to describe geometrically the static equilibrium shape of the boom in terms of its assumed initial, unheated shape and the bending due to thermal radiation. This static equilibrium shape is described in terms of a radius of curvature and the angle between the final plane of bending and some fixed reference. These variables appear in the stability polynomial. The second step is to establish a relationship between the thermal bending moments and the angle of twist of the boom. The details of this step are given in appendix A. The third step is to determine the structural properties of the boom. These take the form of load-deflection relationships. The loads are assumed to be forces acting at the boom tip in a direction normal to the boom axis, a torque acting along the boom axis at the tip, and an arbitrary distribution of bending moments along the boom axis. The appropriate equations are developed in appendix B. The final step is to identify the loads acting on the boom in terms of force of inertia of the tip mass and the thermal bending moments. Four linear differential equations result whose characteristic polynomial defines the stability of the boom system.

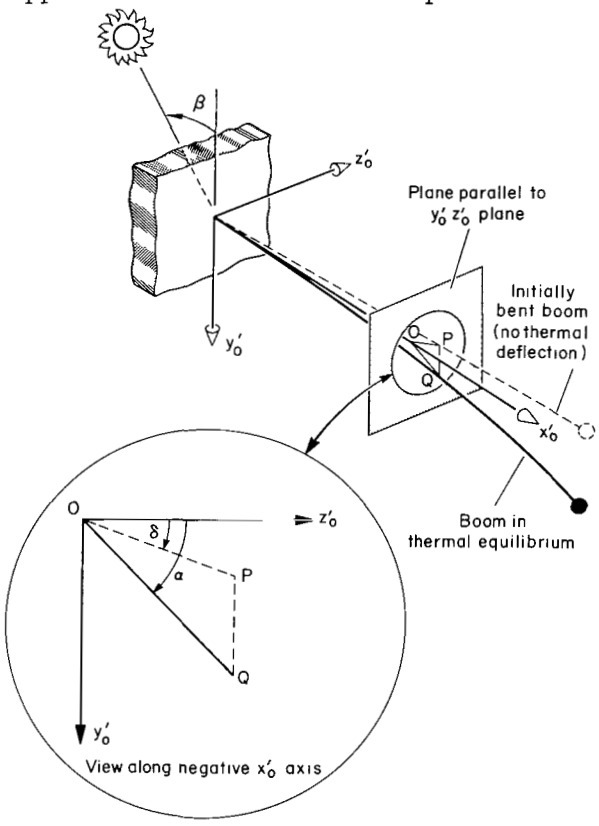

Figure 1.- Boom system (primary coordinates and geometry of deformation).

Principal Assumptions

The boom system to be analyzed and the primary coordinate reference system is shown in figure 1. A precise definition of this coordinate system is given in the Nomenclature.

The following principal assumptions are made about the characteristics of the boom.

1. In the absence of any radiation the centroidal axis of the boom has a constant radius of curvature R_o along the length of the boom. Furthermore, the curvature vector at any point on the boom axis lies in a plane whose normal makes an angle δ to the y_o' axis (see fig. 1).

2. The initial radius of curvature R_o and the thermally induced radius of curvature R_s are both large compared with the boom length L.

3. The boom cross section is circular, thin-walled, thermally seamless, and constant along the length. In addition, the principal second moments of area are equal.

4. Warping of the boom cross section is restrained at the root.

5. The entire mass of the boom system is located at the free end. In practice this means that the tip mass of the boom is large compared with the mass of the boom itself.

6. Boom bending does not substantially change the orientation of the boom relative to the direction of radiation and, therefore, has no influence on thermal bending moments. This assumption places some restrictions on the magnitude of the angle β between the y_o' axis and the direction of the radiation.

7. The centroidal and shear axes of the boom coincide.

8. Thermal torques are negligible.

Several other special assumptions of a less fundamental nature are introduced and defined as they are required in the analysis.

Geometry of the Equilibrium State

The static equilibrium shape of the boom results from the combined effects of its initial shape and a thermally induced bending moment. It follows from equations (A29) that the thermally induced bending moment is constant along the boom axis and acts about the z_o' axis. Simple bending theory shows that the thermally induced equilibrium radius of curvature R_s is constant along the length and the corresponding contribution to the total curvature vector lies in the $x_o'y_o'$ plane. It follows that, to a first approximation, the static equilibrium shape resulting from the combined effects of initial and thermally induced curvatures is planar. This is because for all points along the boom the triangles OPQ, shown in figure 1, are similar. In fact, at any point x along the boom $OP \approx x^2/2R_o$, $PQ \approx x^2/2R_s$, $OQ \approx x^2/2R$, where R is the radius of curvature of the static equilibrium shape, and R_o is the radius of curvature of the initial shape. The geometry shown in figure 1 then yields the following expressions from which the radius of curvature R and the angle α between the normal to the plane of the boom and the y_o' axis may be obtained.

$$\frac{1}{R^2} = \frac{1}{R_o^2} + \frac{1}{R_s^2} + \frac{2 \sin \delta}{R_o R_s} \tag{1}$$

$$\frac{\sin \alpha}{R} = \frac{1}{R_s} + \frac{\sin \delta}{R_o} \tag{2}$$

Thermal Bending Moments and Boom Deflection Equations

Suppose now that the boom system is deflected from its equilibrium by forces $F_y(t)$ and $F_z(t)$ and a torque $T(t)$ (see fig. 2). By assumption (6) the translational deflections y and z cause no changes in the thermal bending moments. On the other hand it is shown in appendix A that a twist deflection ψ does produce changes in the thermal bending moments. It is shown in appendix A that for small angles of twist, the equilibrium thermal bending moment $M_{z''}(\infty)$ remains constant in magnitude. However, if it is assumed that the direction of the $M_{z''}(\infty)$ moment rotates with the cross section, then an additional thermal bending moment $\Delta M_{y'}(x,t)$ whose magnitude is given by equation (A37) acts in the direction of the y' axis. Thus,

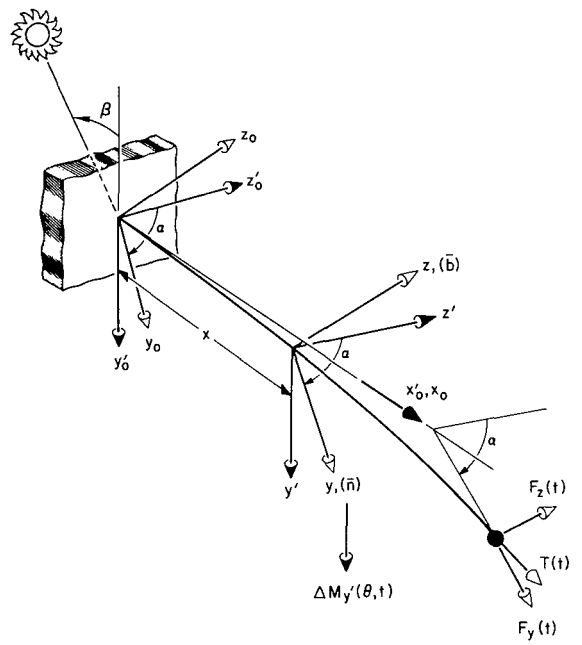

Figure 2.- Boom system (forces and torques).

$$\frac{d\,\Delta M_{y'}(x,t)}{dt} + \lambda\,\Delta M_{y'}(x,t) = \lambda M_{z''}(\infty)\psi(x,t) \tag{3}$$

and from equations (A29) and (A15)

$$M_{z''}(\infty) = \frac{J_s \alpha_s e_c E \pi r^2 \cos \beta}{2\rho c \lambda} \tag{4}$$

$$\lambda = \frac{4\sigma\varepsilon T_o^3}{h\rho c} + \frac{K}{\rho c r^2} \tag{5}$$

where β is the angle between the direction of radiation and the negative y_o' axis (see fig. 1). (Note: since thermal bending moments are associated only with the first thermal mode, the subscript may be deleted from λ_1.)

Equation (3) may be written in the following form

$$\frac{d\eta(x,t)}{dt} + \lambda\eta(x,t) = \lambda\psi(x,t) \tag{6}$$

where

$$\eta(x,t) = \frac{\Delta M_{y'}(x,t)}{M_{z''}(\infty)} \tag{7}$$

Since $M_{z''}(\infty)$ remains constant in magnitude and its direction rotates with the cross section, it follows that its entire effect is equivalent to a permanent bend in the boom. The radius of curvature of the bend, as given by the Bernoulli-Euler bending theory, is

$$\frac{1}{R_s} = \frac{M_{z''}(\infty)}{EI} \tag{8}$$

With $M_{z''}(\infty)$ replaced by this permanent bend, the only thermal bending moment acting on the boom is $\Delta M_{y'}(x,t)$. Since by assumption (8) thermal torques are assumed to be negligible, the load system acting on the boom is as shown in figure 2. The deflections of the boom may be obtained directly from the results of appendix B. It follows from figure 2 that

$$\left.\begin{aligned} \Delta M_b(x,t) &= -\Delta M_{y'}(x,t)\cos\alpha = -\frac{EI}{R_s}\eta(x,t)\cos\alpha \\ \Delta M_\eta(x,t) &= \Delta M_{y'}(x,t)\sin\alpha = \frac{EI}{R_s}\eta(x,t)\sin\alpha \end{aligned}\right\} \tag{9}$$

Incorporating the above relationships into equations (B34), (B35), and (B22) gives the following expressions for $y(L,t)$, $z(L,t)$, and $\psi(L,t)$:

$$y(L,t) = \frac{F_y(t)}{3EI}\left(L^3 - \frac{L^5}{5R^2}\right) - \frac{N(L,t)\cos\alpha}{R_s} \tag{10}$$

$$z(L,t) = F_z(t)\left\{\frac{L^3}{3EI} + \frac{L^5}{5R^2}\left[\frac{f_3(kL)}{4C} - \frac{1}{3EI}\right]\right\} + \frac{T(t)L^3}{3R}\left[\frac{f_1(kL)}{2C} - \frac{1}{EI}\right] - \frac{N(L,t)\sin\alpha}{R_s} \tag{11}$$

$$\psi(L,t) = \frac{F_z(t)L^3}{3R}\left[\frac{f_1(kL)}{2C} - \frac{1}{EI}\right] + \frac{T(t)Lf_2(kL)}{C} + \frac{N(L,t)\sin\alpha}{RR_s} \tag{12}$$

where

$$N(L,t) = R\int_0^L \eta(x,t)\sin\left(\frac{L-x}{R}\right)dx \tag{13}$$

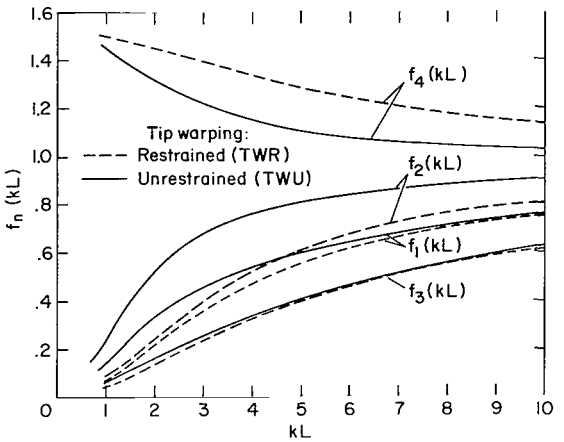

Figure 3.- Variation of $f_1(kL)$, $f_2(kL)$, $f_3(kL)$, and $f_4(kL)$.

and graphs of the functions $f_1(kL)$, $f_2(kL)$, and $f_3(kL)$ are given in figure 3.

Equation (6) is now multiplied by $R \sin[(L - x)/R]$ and integrated with respect to x over the interval $0 \leq x \leq L$. The result is

$$\frac{dN(L,t)}{dt} + \lambda N(L,t) = \lambda R \int_0^L \psi(x,t) \sin\left(\frac{L-x}{R}\right) dx \tag{14}$$

It has been shown in appendix C that over any interval of time starting at zero the maximum angle of twist due to thermal bending moments alone is less than the maximum total angle of twist multiplied by $(x^2/2RR_s)\sin\alpha$. Since, by assumption (2), $(x^2/2RR_s) << 1$, it follows that angle of twist due to thermal bending moments may be neglected without much loss of accuracy. Thus the last term of equation (12) may be deleted along with the last term of equation (B21). This simplification of equation (B21) permits the integral expression in equation (14) to be evaluated explicitly. Thus, the integral can be written in the form

$$R \int_0^L \psi(x,t) \sin\left(\frac{L - x}{R}\right) dx = R \int_0^L [\psi_T(x,t) + \psi_B(x,t)] \sin\left(\frac{L - x}{R}\right) dx \tag{15}$$

where $\psi_T(x,t)$ and $\psi_B(x,t)$ are defined in appendix B. Therefore by equations (B31) and (B32), equation (15) becomes

$$R \int_0^L \psi(x,t) \sin\left(\frac{L-x}{R}\right) dx = \frac{F_z(t) L^5 f_3(kL)}{20RC} + \frac{T(t) L^3 f_1(kL)}{6C} + R \int_0^L \psi_B(x,t) \sin\left(\frac{L-x}{R}\right) dx \tag{16}$$

Substituting for $\psi_B(x,t)$ from equation (B21) into equation (16) gives the following final form of equation (14)

$$\frac{dN(L,t)}{dt} + \lambda N(L,t) = \frac{\lambda F_z(t) L^5}{10R} \left[\frac{f_3(kL)}{2C} - \frac{1}{3EI}\right] + \frac{\lambda T(t) L^3 f_1(kL)}{6C} \tag{17}$$

Equations (10), (11), (12), and (17) are the final complete set of boom deflection equations.

The Characteristic Stability Polynomial

If the boom system has no external forces acting on it, the forces $F_y(t)$, $F_z(t)$ and torque $T(t)$ are due entirely to mass-accelerations and internal structural damping and may be represented as follows:

$$F_y(t) = -m_T \frac{d^2y(L,t)}{dt^2} - D_y \frac{dy(L,t)}{dt} \tag{18}$$

$$F_z(t) = -m_T \frac{d^2z(L,t)}{dt^2} - D_z \frac{dz(L,t)}{dt} \tag{19}$$

$$T(t) = -I_\psi \frac{d^2\psi(L,t)}{dt^2} - D_\psi \frac{d\psi(L,t)}{dt} \tag{20}$$

where

m_T tip mass

I_ψ tip inertia about the boom axis

D_y, D_z, D_ψ effective structural damping for translation along $\bar{b}(L)$ and $\bar{n}(L)$ and rotation about $\bar{t}(L)$, respectively

Equations (10), (11), (12), (17), (18), (19), and (20) form the complete set of linearized dynamical equations from which $F_y(t)$, $F_z(t)$, and $T(t)$ may be eliminated to yield four equations in the variables $y(L,t)$, $z(L,t)$, $\psi(L,t)$, and $N(L,t)$. These equations describe the motion of the boom system under the sole influence of the thermoelastic effects due to thermal radiation. The characteristic polynomial is given below in determinant form where the symbol "s" is used to denote the Laplace transform variable. The columns of the determinant correspond to the variables $y(L,t)$, $z(L,t)$, $\psi(L,t)$, and $N(L,t)$, respectively. The first two rows correspond to the y and z translational equations of motion of the tip, the third row to the rotational equation of motion of the tip about the boom axis and the fourth row to the dynamic relationship between thermal bending moments and angle of twist.

$$\begin{vmatrix} (m_T s^2 + D_y s)\left(1 - \frac{L^2}{5R^2}\right)\frac{L^3}{3EI} + 1 & 0 & 0 & \frac{\cos\alpha}{R_s} \\ 0 & (m_T s^2 + D_z s)\left\{\frac{L^3}{3EI} + \frac{L^5}{5R^2}\left[\frac{f_3(kL)}{4C} - \frac{1}{3EI}\right]\right\} + 1 & (I_\psi s^2 + D_\psi s)\left[\frac{f_1(kL)}{2C} - \frac{1}{EI}\right]\frac{L^3}{3R} & \frac{\sin\alpha}{R_s} \\ 0 & (m_T s^2 + D_z s)\left[\frac{f_1(kL)}{2C} - \frac{1}{EI}\right]\frac{L^3}{3R} & (I_\psi s^2 + D_\psi s)\frac{Lf_2(kL)}{C} + 1 & 0 \\ 0 & (m_T s^2 + D_z s)\left[\frac{f_3(kL)}{2C} - \frac{1}{3EI}\right]\frac{L^5\lambda}{10R} & (I_\psi s^2 + D_\psi s)\frac{L^3 f_1(kL)\lambda}{6C} & s + \lambda \end{vmatrix} = 0 \tag{21}$$

One solution of equation (21) is

$$(m_T s^2 + D_y s)\left(1 - \frac{L^2}{5R^2}\right)\frac{L^3}{3EI} + 1 = 0 \tag{22}$$

This is a damped mode of oscillation for any positive values of D_y. It cannot exhibit instability and is therefore not considered further. The stability of the remaining modes of motion is given by the remaining solutions of equation (21):

$$\begin{vmatrix} (m_T s^2 + D_z s)\left\{\frac{L^3}{3EI} + \frac{L^5}{5R^2}\left[\frac{f_3(kL)}{4C} - \frac{1}{3EI}\right]\right\} + 1 & (I_\psi s^2 + D_\psi s)\left[\frac{f_1(kL)}{2C} - \frac{1}{EI}\right]\frac{L^3}{3R} & \frac{\sin\alpha}{R_s} \\ (m_T s^2 + D_z s)\left[\frac{f_1(kL)}{2C} - \frac{1}{EI}\right]\frac{L^3}{3R} & (I_\psi s^2 + D_\psi s)\frac{Lf_2(kL)}{C} + 1 & 0 \\ (m_T s^2 + D_z s)\left[\frac{f_3(kL)}{2C} - \frac{1}{3EI}\right]\frac{L^5\lambda}{10R} & (I_\psi s^2 + D_\psi s)\frac{L^3 f_1(kL)\lambda}{6C} & s + \lambda \end{vmatrix} = 0 \tag{23}$$

ANALYSIS OF THE STABILITY POLYNOMIAL

In this section the stability polynomial, given by equation (23), is analyzed to obtain the maximum degree of instability and conditions for stability. Two types of boom cross section are considered. The first is the structurally seamless cross section which has the important characteristic that the torsional and flexural rigidities are of the same order of magnitude. The ratio of the two is given by the expression

$$\frac{C}{EI} = \frac{1}{1 + \nu} \tag{24}$$

where ν is Poisson's ratio. For most materials Poisson's ratio is close to 1/3 and, when specific numerical results are given, this is the value that will be assumed. The second cross section considered is the open overlapped type used in most space applications. The important structural characteristic of this cross section is that the torsional stiffness is much smaller than the bending stiffness. This may be expressed in the form

$$\frac{C}{EI} << 1 \tag{25}$$

System Stability in the Absence of Structural Damping

When $D_\psi = D_Z = 0$, equation (23) can be written in the form

$$\begin{vmatrix} m_T s^2 A + 1 & I_\psi s^2 D & 1 \\ m_T s^2 D & I_\psi s^2 F + 1 & 0 \\ m_T s^2 B\lambda & I_\psi s^2 G\lambda & s + \lambda \end{vmatrix} = 0 \tag{26}$$

where

$$A \triangleq \frac{L^3}{3EI} + \frac{L^5}{5R^2}\left[\frac{f_3(kL)}{4C} - \frac{1}{3EI}\right] \tag{27}$$

$$B \triangleq \left[\frac{f_3(kL)}{2C} - \frac{1}{3EI}\right]\frac{L^5 \sin \alpha}{10RR_s} \tag{28}$$

$$D \triangleq \left[\frac{f_1(kL)}{2C} - \frac{1}{EI}\right]\frac{L^3}{3R} \tag{29}$$

$$F \triangleq \frac{L}{C} f_2(kL) \tag{30}$$

$$G \triangleq \frac{L^3 f_1(kL) \sin \alpha}{6R_s C} \tag{31}$$

Equation (26), in its expanded form, is

$$s^5 m_T I_\psi (AF - D^2) + s^4 m_T I_\psi \lambda [D(G - D) + F(A - B)]$$

$$+ s^3(m_T A + I_\psi F) + s^2\lambda[m_T(A - B) + I_\psi F] + s + \lambda = 0 \tag{32}$$

It is shown in reference 5 that any fifth-order polynomial

$$a_o s^5 + a_1 s^4 + a_2 s^3 + a_3 s^2 + a_4 s + a_5 = 0$$

has stable roots if and only if all the coefficients are the same sign and the following two inequalities are also satisfied simultaneously

$$\left.\begin{aligned} a_1 a_2 - a_0 a_3 &> 0 \\ (a_1 a_2 - a_0 a_3)(a_3 a_4 - a_2 a_5) - (a_1 a_4 - a_0 a_5)^2 &> 0 \end{aligned}\right\} \tag{33}$$

It follows from equation (32) that

$$a_3a_4 - a_2a_5 = -m_T B\lambda$$

Therefore when $B > 0$

$$a_3a_4 - a_2a_5 < 0 \tag{34}$$

However, if condition (34) holds then conditions (33) cannot hold simultaneously. Therefore the system is unstable. In particular, for initially straight booms of either seamless or open cross section $B > 0$. These initially straight booms are therefore always unstable in the absence of structural damping.

Conditions Under Which I_ψ May Be Neglected

Consider the case of a boom not under the influence of thermal radiation but still bent into a circular arc of radius R. The coupled flexural-torsional dynamical behavior of this boom would be described by the translational equation of motion in the z direction and the rotational equation of motion about the boom axis. Since heating is absent, the variable N and the thermal bending moment equation need not be included. The frequencies of the natural undamped modes of vibration ($D_z = D_\psi = 0$) are therefore given by the first two rows and columns of the determinant in equation (26);

$$\begin{vmatrix} m_T A s^2 + 1 & I_\psi D s^2 \\ m_T D s^2 & I_\psi F s^2 + 1 \end{vmatrix} = 0 \tag{35}$$

Equation (35) may be expanded into the form

$$m_T I_\psi (AF - D^2)s^4 + (I_\psi F + m_T A)s^2 + 1 = 0 \tag{36}$$

If I_ψ is to have an insignificant effect on the frequency of the mode associated with m_T and which, in an unbent boom, would be the flexural mode, the polynomial $m_T A s^2 + 1$ must be an approximate factor of equation (35). It can be shown, by dividing equation (36) by $m_T A s^2 + 1$, that this is true if and only if

$$\frac{I_\psi}{m_T}\left(\frac{D}{A}\right)^2 << 1$$

A good working rule, therefore, might be that I_ψ has very little influence on the flexural frequency if

$$I_\psi \leq \frac{m_T}{10}\left(\frac{A}{D}\right)^2 \tag{37}$$

If ρ_ψ is the radius of gyration of the tip mass about the axis of the boom, then inequality (37) can be written in the form

$$\rho_\psi \leq \frac{1}{\sqrt{10}} \left|\frac{A}{D}\right| \tag{38}$$

It will be demonstrated, in the sequel, that the influence of thermal radiation is to produce an unstable mode with a frequency close to that given by $m_T A s^2 + 1 = 0$. It is also clear that reasonable amounts of structural damping will not have a great influence on the frequency of this unstable mode. Therefore inequality (38), which indicates when I_ψ does not influence the natural structural mode of frequency $\sqrt{1/m_T A}$, should also give a rough indication of when I_ψ does not influence the thermally induced instability of a boom possessing some structural damping.

For a boom with a structurally seamless cross section $k = \infty$, so that $f_1(kL) = f_2(kL) = f_3(kL) = 1$, and the expressions for A and D given by equations (27) and (29) become (with $\nu = 1/3$)

$$A = \frac{L^3}{3EI}$$

$$D = -\frac{L^3}{9REI}$$

Inequality (38) then becomes

$$\rho_\psi \leq \frac{3R}{\sqrt{10}} \approx R \tag{39}$$

Most booms have a value of R greater than 100 m so that it is clear from inequality (39) that, for most practical boom systems employing structurally seamless cross sections, the tip inertia I_ψ will have a negligible effect on boom dynamics.

For a boom with an open cross section, A and D become

$$A = \frac{L^3}{3EI} + \frac{L^5 f_3(kL)}{20R^2C}$$

$$D = \frac{L^3 f_1(kL)}{6RC}$$

Inequality (38) then becomes

$$\rho_\psi \leq \frac{1}{\sqrt{10}} \frac{\frac{L^3}{3EI} + \frac{L^5 f_3(kL)}{20R^2C}}{\frac{L^3 f_1(kL)}{6RC}} \tag{40}$$

The requirements on ρ_ψ given by inequality (40) are most stringent when $C \to 0$. Also the ratio $f_3(kL)/f_1(kL)$ is close to unity for most booms. Thus I_ψ cannot influence the dynamics of booms with open cross section ($C/EI \ll 1$) if

$$\rho_\psi \leq \frac{3}{10\sqrt{10}} \frac{L^2}{R} \approx \frac{L^2}{10R} \tag{41}$$

It can be seen by comparing inequalities (39) and (41) that the limiting value of ρ_ψ for a boom with an open cross section is much less than that for a boom with a seamless cross section. In fact, the ratio of the two is $(1/10)(L/R)^2$. Even though the limiting value of ρ_ψ indicated by inequality (41) can be quite low, it has never been exceeded in boom systems used for space applications. Consequently, for the remainder of the analytical treatment given in this report it is assumed that $I_\psi = 0$. It is conceivable, however, that future boom systems may employ tip masses with rotational inertias large enough to influence the boom dynamics. In these cases the complete polynomial, given by equation (23), must be used in evaluating the stability.

The Influence of Flexural Damping D_z

Some of the implications of equation (23) can be best understood by a study of the system with no rotational inertia or rotational damping. With $I_\psi = D_\psi = 0$ equation (23) reduces to

$$m_T A s^3 + [D_z A + m_T \lambda (A - B)]s^2 + [1 + D_z \lambda (A - B)]s + \lambda = 0 \tag{42}$$

For a seamless cross section, equation (24) and $L^2/R^2 \ll 1$, permit equations (27) and (28) to be simplified:

$$A = \frac{L^3}{3EI} \tag{43}$$

$$B = \frac{(1 + 3\nu)L^5 \sin \alpha}{60EIRR_s} \qquad f_3(kL) = 1 \tag{44}$$

For a split cross section using inequality (25), the corresponding expressions are

$$A = \frac{L^3}{3EI} + \frac{L^5 f_3(kL)}{20CR^2} \tag{45}$$

$$B = \frac{L^5 f_3(kL)\sin\alpha}{20CRR_s} \tag{46}$$

From the points of view of both analysis and presentation of computational results, a more convenient form of equation (42) is obtained by expressing it in terms of the following set of dimensionless parameters:

$$\lambda^* \triangleq \lambda\sqrt{m_T(A - B)} \tag{47}$$

$$s^* \triangleq s\sqrt{m_T(A - B)} \tag{48}$$

$$\zeta_z \triangleq \frac{D_z}{2m_T}\sqrt{m_T(A - B)} \tag{49}$$

$$X \triangleq \frac{B}{A} \tag{50}$$

It should be noted that ζ_z is the flexural damping factor based on a circular frequency $\sqrt{m_T(A - B)}$. Normally the flexural damping factor ζ_z' is based on the natural undamped circular frequency in flexure $\sqrt{m_T L^3/3EI}$. The conversion from one to the other is therefore

$$\zeta_z' = \zeta_z\sqrt{\frac{L^3}{3EI(A - B)}}$$

The dimensionless form of equation (42) corresponding to the dimensionless parameters defined above is

$$\frac{s^{*3}}{1 - X} + \left(\frac{2\zeta_z}{1 - X} + \lambda^*\right)s^{*2} + (1 + 2\lambda^*\zeta_z)s^* + \lambda^* = 0 \tag{51}$$

It is shown in reference 5 that any cubic equation

$$a_0 s^3 + a_1 s^2 + a_2 s + a_3 = 0$$

has stable roots if and only if all the coefficients have the same sign and

$$a_1 a_2 > a_0 a_3 \tag{52}$$

Inequality (52) written in terms of the coefficients of equation (51) becomes

$$\zeta_z^2 + \frac{\zeta_z}{2\lambda^*}\left[1 + \lambda^{*2}(1 - X)\right] - \frac{X}{4} > 0 \tag{53}$$

If no structural damping is present ($\zeta_z = 0$) the stability criteria can be satisfied if and only if $X < 0$. It follows from the definition of X that this condition is equivalent to $\sin\alpha < 0$ or $0 > \alpha > -\pi$. Therefore stability or instability will prevail according to whether or not the boom, in static equilibrium, and the radiation source are both on the same side of a plane passing through the boom root perpendicular to the direction of radiation. This condition for stability may be interpreted in terms of a relationship between the direction and magnitude of the initial curvature and the thermally induced curvature. Thus, from equation (2), if $(\sin\delta/R_o) < -(1/R_s)$ the boom will be stable and if $(\sin\delta/R_o) > -(1/R_s)$ the boom will be unstable. In particular, if the boom is initially straight, then $(1/R_o) = 0$, and it is always unstable. The instability can occur in two forms, depending on the value of X. This can be seen more clearly if equation (51), with $\zeta_z = 0$, is expressed in the standard root locus form

$$1 + [\lambda^*(1 - X)]\frac{(s^{*2} + 1)}{s^*(s^{*2} + 1 - X)} = 0$$

in which $\lambda^*(1 - X)$ is the gain factor.

The root locus for $0 < X < 1$ differs from that for $1 < X < \infty$ as can be seen from figure 4. Thus when $0 < X < 1$ the instability is always an oscillatory divergence; whereas when $1 < X < \infty$ the instability may be a pure divergence of the type associated with static instability.

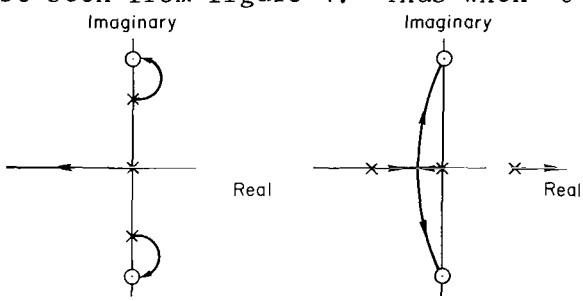

(a) $0 < X < 1$ (b) $1 < X < \infty$

Figure 4.- Root Loci for $X > 0$.

It follows from equations (43) and (44) that the value of X for a boom with a seamless cross section can never exceed $[(1 + 3\nu)L^2 \sin\alpha]/20RR_s$, which is small compared with unity. For such a boom, therefore, any instability must always be of the oscillatory or flutter type. This same statement, however, cannot be made for booms of open cross section. In this case it follows from equations (45) and (46) that

$$X = \frac{\frac{3}{20}\frac{EI}{C}\frac{L^2 f_3(kL)\sin\alpha}{RR_s}}{1 + \frac{3}{20}\frac{EIL^2 f_3(kL)}{CR^2}} \tag{54}$$

If $1/R^2$ and $\sin\alpha/R$, given by equations (1) and (2), respectively, are substituted into equation (54), there results an expression for X in terms of

R_o and δ. The maximum value of X with respect to R_o and δ is given by

$$X = \frac{1}{2R_s}\sqrt{\frac{3EIL^2 f_3(kL)}{20C}}$$

This maximum occurs when $\delta = -\pi/2$ and

$$\frac{1}{R_o} = \frac{1}{R_s} - \sqrt{\frac{20C}{3EIL^2 f_3(kL)}}$$

Clearly, therefore, as $EI/C \to \infty$, $X \to \infty$. However, from equation (54), if the values of R_o and δ satisfy the inequality

$$\frac{1}{R_o}\left(\frac{\sin\delta}{R_s} + \frac{1}{R_o}\right) \geq \frac{-20C}{3EIL^2 f_3(kL)}$$

then $X \leq 1$. This condition on R_o and δ is not too stringent and, in particular, holds for initially straight booms. It is anticipated that most practical boom systems will satisfy the above condition on R_o and δ, which is therefore assumed to hold throughout the remainder of this report. The report is therefore concerned only with the oscillatory instabilities associated with values of X in the interval $0 < X \leq 1$.

It is of interest to know the greatest degree of instability that can occur, as measured by magnitude of the real part of the divergent roots of equation (51). The answer to this question depends on which of the two variables λ^*, X is maintained constant. Both cases, namely, variable λ^* at a fixed X and variable X at a fixed λ^* are treated in appendix D. When $\zeta_z = 0$ and X is constant, the real part of the divergent root has a maximum value given by

$$p^* = \frac{X}{4} \tag{55}$$

and this occurs at a value of λ^* given by

$$\lambda^* = \frac{2 - X}{2(1 - X)} \tag{56}$$

with the corresponding imaginary part of the root given by

$$q^* = \sqrt{1 - \frac{X}{2} - \frac{X^2}{16}} \tag{57}$$

These results may be expressed in dimensional form and simplified for the case of a boom with a seamless cross section by substituting for A and B from equations (43) and (44) and using the condition that $X << 1$. The results, in dimensional form (see notation for definition of p^* and q^*), are

$$p = \frac{L^2(1 + 3\nu)\sin \alpha}{80RR_s} \sqrt{\frac{3EI}{m_T L^3}} \tag{58}$$

$$\lambda \approx q \approx \sqrt{\frac{3EI}{m_T L^3}} \tag{59}$$

Equations (58) and (59) show that since $L^2 \sin \alpha/RR_s << 1$ the frequency of the divergent mode is approximately equal to the frequency of the flexural mode of a straight boom. The instability will therefore appear to an observer as if the boom were oscillating in both bending and torsion at its natural bending frequency, and diverging as if it had a damping factor equal to $[-L^2(1 + 3\nu)\sin \alpha]/80RR_s$. If $1/R_o > 1/R_s$ this quantity has a lower bound of $[-(1 + 3\nu)/40](L^2/R_s{}^2)$. With $\nu = 1/3$ and $L/R_s = 0.1$ this lower bound has a value of -0.0005. This is clearly a mild divergence. The basic reason why booms with seamless cross section can exhibit only a mild divergence is that, because the torsional and bending stiffnesses are of the same order of magnitude, $X = B/A$ is always small. This is not the case when the torsional stiffness is low compared with the bending stiffness, as for a boom of open cross section. Thus, for example, equation (54) shows that, for an initially straight boom ($1/R_o = 0$), $X \to 1$ as $EI/C \to \infty$.

When $\zeta_z = 0$, it follows from the results of appendix D that, for a fixed value of λ^*, the maximum value of the real part of the divergent root is (eq. (D29))

$$p^* = \frac{\lambda^*}{2(1 + 2\lambda^*)} \tag{60}$$

and this occurs at a value of X given by (eq. (D30))

$$X = 1 - \frac{\lambda^*}{(1 + \lambda^*)(1 + 2\lambda^*)} \tag{61}$$

with the corresponding imaginary part of the root given by (eq. (D32) using eqs. (60) and (D28))

$$q^* = \sqrt{\frac{\lambda^*(4 + 7\lambda^*)}{4(1 + 2\lambda^*)^2}} \tag{62}$$

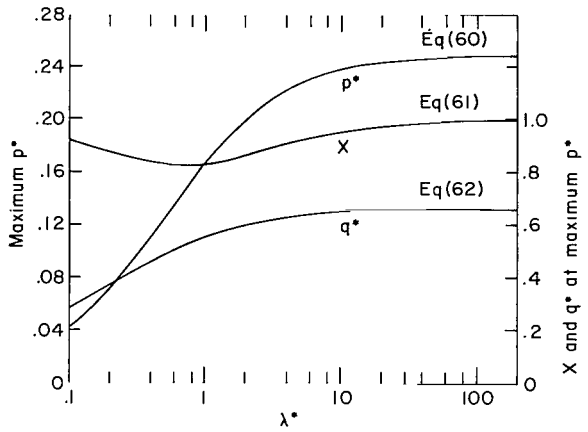

Figure 5.- Variation of maximum real part of unstable root (p*) with λ^*.

Graphs of equations (60), (61), and (62) are given in figure 5.

It follows from equations (60), (61), and (62) that p^* attains its maximum value when $\lambda^* \to \infty$. In the limit

$$\lim_{\lambda^* \to \infty} p^* = \frac{1}{4} \tag{63}$$

$$\lim_{\lambda^* \to \infty} X = 1 \tag{64}$$

$$\lim_{\lambda^* \to \infty} q^* = \sqrt{\frac{7}{16}} \tag{65}$$

For the case of an initially straight boom ($1/R_o = 0$) the corresponding limiting dimensional values of the unstable roots are

$$p = \frac{1}{4}\sqrt{\frac{3EI}{m_T L^3}} \tag{66}$$

$$q = \sqrt{\frac{7}{16}}\sqrt{\frac{3EI}{m_T L^3}} \tag{67}$$

It follows from equations (66) and (67) that

$$p = \frac{\sqrt{2}}{4}\sqrt{p^2 + q^2} \tag{68}$$

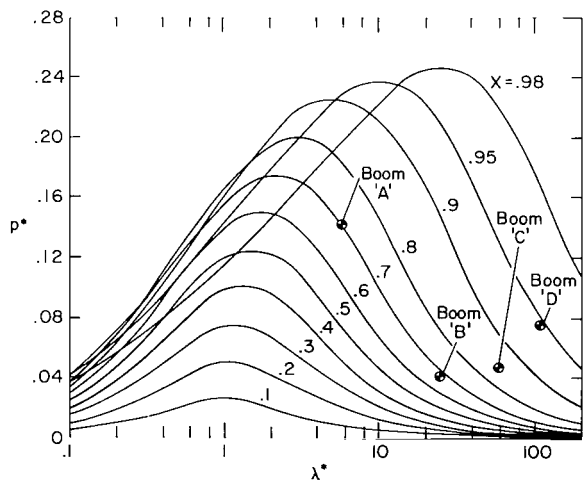

Figure 6.- Variation of real part of unstable root (p*), with λ^*, for various values of X.

where $\sqrt{p^2 + q^2}$ is the circular frequency of the unstable oscillation. To an observer, therefore, a boom for which $X \to 1$ and $\lambda^* \to \infty$ will appear to oscillate in both bending and torsion with a frequency that is about 66 percent of the natural bending frequency of a straight boom. It will also appear to be diverging as if it had a damping factor equal to $-\sqrt{2}/4$ or -0.354. This is clearly a rapid divergence. Furthermore, it remains severe down to quite a small value of λ^*. For example, it is shown in figure 5 that if $\lambda^* > 2$, then $p^* > 0.2$. To complete the survey of the instabilities shown by equation (51) the variation of p^* with λ^* for various values of X is shown in figure 6. This graph shows the two types of maxima for p^* which have been discussed.

It is important to note here that the effect of boom tip condition on stability is dictated by the function $f_3(kL)$ (see eq. (54)). It follows from figure 3 that, for values of kL greater than about 2, the stability of a boom is independent of whether or not the tip is restrained from warping.

For a fixed value of X the amount of flexural damping ζ_z required to stabilize the boom for all values of λ^* may be determined by setting $p^* = 0$ in equation (D16). The result is

$$\zeta_z = \frac{1}{2} - \frac{1}{2}\sqrt{1 - X} \tag{69}$$

and occurs at the following value of λ^* obtained by substituting equation (69) into equation (D17),

$$\lambda^* = \frac{1}{\sqrt{1 - X}} \tag{70}$$

with the corresponding imaginary part of the root given by

$$q^{*2} = \sqrt{1 - X} \tag{71}$$

Alternatively, equations (69) and (70) may be obtained by differentiating equation (53) with respect to λ^* and setting $\partial\zeta_z/\partial\lambda^* = 0$.

For a boom with a seamless cross section equations (69), (70), and (71) become, using equations (43) and (44),

$$\zeta_z = \frac{L^2(1 + 3\nu)\sin\alpha}{80RR_s} \tag{72}$$

$$\lambda \approx q \approx \sqrt{\frac{3EI}{m_T L^3}} \tag{73}$$

These results compared with equations (58) and (59) show that the structural damping required to counter the boom instability is equal to the magnitude of the effective negative damping factor corresponding to the maximum instability when the boom has no structural damping. The value of ζ_z given by equation (72) is very small and will probably be exceeded by the structural damping present in most practical boom systems employing seamless cross-section members. It is, therefore, unlikely that instability will ever be observed in these types of boom.

The maximum structural damping required for stability when λ^* is assumed constant occurs when $X = 1$. This can be shown from equations (D29) and (D30) of appendix D, from which it also follows that

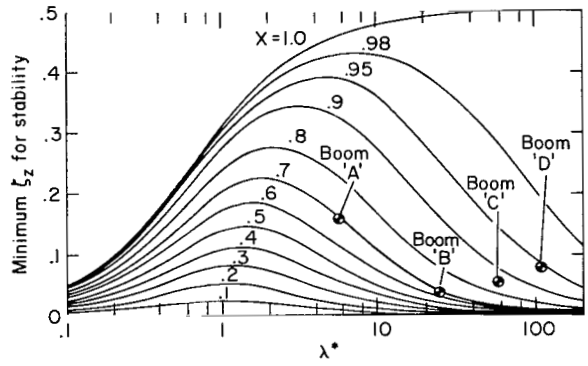

Figure 7.- Minimum flexural damping (ζ_z) required for stability.

$$\zeta_z = \frac{-1 + \sqrt{1 + 4\lambda^{*2}}}{4\lambda^*} \tag{74}$$

for $p^* = 0$. The corresponding value for the imaginary part of the root is $q^* = 0$. In other words the oscillation is "dead beat." The graph of equation (74) is plotted in figure 7 along with the variation of ζ_z with λ^* for other values of X. Since for a boom with an open cross section X can approach unity, it is clear that large values of ζ_z may be required. In particular, if $\lambda^* > 2$ then $\zeta_z > 0.4$. The asymptotic value of ζ_z for $X = 1$ is 0.5. This therefore represents the ζ_z which will stabilize a boom with a circular thin-wall cross section irrespective of the material it is made from, the initial curvature, or the L/R_s ratio. It is interesting to note that the ζ_z required to stabilize the worst case instabilities is somewhat greater than the negative damping factor of the instability when $\zeta_z = 0$.

The Influence of Torsional Damping D_ψ

It has been demonstrated in the last section that it is unlikely that instabilities of booms with seamless cross sections will ever be observed. The following treatment, to determine the influence of torsional damping, is therefore restricted to the more unstable open cross-section boom configurations characterized by $EI/C >> 1$. Consider the case wherein $D_z = I_\psi = 0$ and the boom is initially straight ($1/R_o = 0$). The stability polynomial (eq. (23)) then reduces to

$$\frac{2}{9}\zeta_\psi\left[9 - \frac{5X_o f_4(kL)}{1 - X_o}\right]s_o^{*4} + \left(\frac{1}{1 - X_o} + 2\zeta_\psi\lambda_o^*\right)s_o^{*3} + (\lambda_o^* + 2\zeta_\psi)s_o^{*2} + (2\zeta_\psi\lambda_o^* + 1)s_o^* + \lambda_o^* = 0 \tag{75}$$

where

$$\zeta_\psi = \frac{D_\psi L f_2(kL)}{2C}\sqrt{\frac{3EI}{m_T L^3}} \tag{76}$$

$$X_o = \frac{\frac{3}{20}\frac{EI}{C}\frac{L^2}{R^2}f_3(kL)}{1 + \frac{3}{20}\frac{EI}{C}\frac{L^2}{R^2}f_3(kL)} \tag{77}$$

$$\lambda_o^* = \lambda\sqrt{\frac{m_T L^3}{3EI}} \tag{78}$$

$$s_o^* = s\sqrt{\frac{m_T L^3}{3EI}} \tag{79}$$

$$f_4(kL) = \frac{[f_1(kL)]^2}{f_2(kL)f_3(kL)}$$

Note that X_o, λ_o^*, and s_o^* are the values of X, λ^*, and s^*, respectively, for an initially straight boom. The graph of $f_4(kL)$ is given in figure 3.

It is shown in reference 5 that any fourth-order polynomial

$$a_0 s^4 + a_1 s^3 + a_2 s^2 + a_3 s + a_4 = 0$$

has stable roots if and only if all the coefficients are positive and

$$a_3(a_1 a_2 - a_0 a_3) - a_4 a_1^2 > 0 \tag{80}$$

In this instance this condition reduces to

$$8[9 - 5f_4(kL)]\lambda_o^{*2}\zeta_\psi^3 + 4[9 - 10f_4(kL)]\lambda_o^*\zeta_\psi^2 - [10f_4(kL) - 18\lambda_o^{*2}]\zeta_\psi + \frac{9\lambda_o^*}{1 - X_o} < 0 \tag{81}$$

This inequality defines a stability boundary which divides the X_o, λ_o^* space into two regions. These are characterized by whether or not the stability condition can be satisfied by a real positive value of ζ_ψ. If the stability condition can be satisfied, then the system can be stabilized by torsional damping; otherwise it cannot. This stability boundary has been calculated for several values of $f_4(kL)$ and is shown in figure 8 with the values of ζ_ψ along the boundary. The cubic equation in ζ_ψ defining the boundary has two equal real positive roots and one real negative root. In the left hand region of figure 8 there are usually two real positive, but unequal, roots and one negative real root. The boom system can then be stabilized only for values of ζ_ψ in the closed interval defined by the two positive roots. In other words, if the torsional damping is gradually increased, the boom system will become stable, but a point will be reached when further increase of torsional damping will result in instability. In the right hand region there is always a real negative root and a pair of complex conjugate roots. In this region, therefore, torsional damping will never stabilize the boom system.

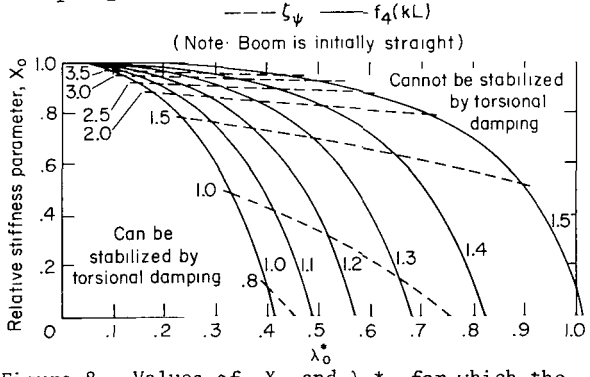

Figure 8.- Values of X_o and λ_o^* for which the boom can be stabilized by torsional damping.

It follows from figure 8 that boom systems characterized by values of X_o close to unity can only be stabilized by torsional damping for very low values of λ_o^* (long thermal time constants). It is clear that, in general, torsional damping is less effective than flexural damping. In fact, figure 7 shows that there is no region of the X, λ^* region which cannot be stabilized by flexural damping.

ANALYSIS OF THE EFFECTIVENESS OF A PASSIVE TIP DAMPER

One way to damp the boom system and, therefore, possibly to stabilize it is to incorporate a damping mechanism in the end mass. A relatively simple scheme is to make the end mass in the form of a thin closed shell containing a viscous fluid and a ball. A disturbance of the boom system then causes relative motion between the spherical shell, attached rigidly to the boom, and the ball residing inside. The motion of the ball through the fluid then dissipates the disturbance energy. Since the ball is free to both rotate and translate, the damping scheme provides both torsional and flexural damping. However, it has been shown that torsional damping is not particularly effective in stabilizing the boom system. Therefore in this analysis it is assumed that the ball motion is one of translation only and the damping effectively confined to the flexural mode. The analysis is further simplified by assuming that $I_\psi = D_\psi = D_z = 0$ (where, it will be recalled, D_ψ and D_z refer to structural damping only) and the mass of the damper fluid is negligible.

The equations of motion of the damper ball along the y and z axis are

$$\left.\begin{aligned} m_d\left[\frac{d^2y(t)}{dt^2} + \frac{d^2y_d(t)}{dt^2}\right] &= -\kappa\,\frac{dy_d(t)}{dt} \\ m_d\left[\frac{d^2z(t)}{dt^2} + \frac{d^2z_d(t)}{dt^2}\right] &= -\kappa\,\frac{dz_d(t)}{dt} \end{aligned}\right\} \tag{82}$$

where

m_d mass of the damper ball

$y_d(t), z_d(t)$ coordinates of the center of mass of the damper ball measured from center of mass of hollow container

κ damping constant (a force of κv is required to move the damper ball through the fluid with velocity v)

The boom alone (less damper ball) force equations as given by equations (18) and (19) must be changed to include the forces exerted by the damper ball. Thus they become

$$F_y(t) = -m_s \frac{d^2y(t)}{dt^2} + \kappa \frac{dy_d(t)}{dt} \tag{83}$$

$$F_z(t) = -m_s \frac{d^2z(t)}{dt^2} + \kappa \frac{dz_d(t)}{dt} \tag{84}$$

where m_s is the mass of the damper shell fixed rigidly to the end of the boom.

Combining equations (82) to (84) with equations (10), (11), (12), and (17) gives the characteristic polynomial which, like equation (21), has two factors. As before one of these is damped and need not be considered further. The other factor is

$$\begin{vmatrix} m_s s^2\left\{\frac{L^3}{3EI} + \frac{L^5}{5R^2}\left[\frac{f_3(kL)}{4C} - \frac{1}{3EI}\right]\right\} + 1 & 0 & \frac{\sin\alpha}{R_s} & -\kappa_s\left\{\frac{L^3}{3EI} + \frac{L^5}{5R^2}\left[\frac{f_3(kL)}{4C} - \frac{1}{3EI}\right]\right\} \\ m_s s^2\left[\frac{f_1(kL)}{2C} - \frac{1}{EI}\right]\frac{L^3}{3R} & 1 & 0 & -\kappa_s\left[\frac{f_1(kL)}{2C} - \frac{1}{EI}\right]\frac{L^3}{3R} \\ m_s s^2\left[\frac{f_3(kL)}{2C} - \frac{1}{3EI}\right]\frac{L^5\lambda}{10R} & 0 & s + \lambda & -\kappa_s\left[\frac{f_3(kL)}{2C} - \frac{1}{3EI}\right]\frac{L^5\lambda}{10R} \\ m_d s & 0 & 0 & m_d s + \kappa \end{vmatrix} = 0 \tag{85}$$

If $P(s, m_s)$ is the polynomial in s formed from the first three rows and three columns of the above determinant, then it follows that equation (85) can be expressed in the form

$$sm_d P(s,m_s) + \kappa P(s,m_s + m_d) = 0 \tag{86}$$

It should be noted that $P(s,m_s)$ is identical to the left hand side of equation (42) when m_T is replaced by m_s and D_z set equal to zero. Equation (86) can therefore be written in the form

$$sm_d[m_s A s^3 + m_s\lambda(A - B)s^2 + s + \lambda]$$
$$+ \kappa[(m_s + m_d)As^3 + (m_s + m_d)\lambda(A - B)s^2 + s + \lambda] = 0 \tag{87}$$

It is convenient at this stage to write this equation in terms of the dimensionless parameters given by definitions (47), (48), and (50) (where $m_T = m_d + m_s$) plus those defined as follows:

$$m_d^* \triangleq \frac{m_d}{m_T} \tag{88}$$

$$\kappa^* \triangleq \kappa \frac{\sqrt{m_T(A - B)}}{m_d} \tag{89}$$

Equation (87) then becomes

$$s^*\left[\frac{(1 - m_d^*)}{1 - X} s^{*3} + (1 - m_d^*)\lambda^* s^{*2} + s^* + \lambda^*\right] + \kappa^*\left(\frac{s^{*3}}{1 - X} + s^{*2}\lambda^* + s^* + \lambda^*\right) = 0 \qquad (90)$$

or

$$\left(\frac{1 - m_d^*}{1 - X}\right) s^{*4} + \left[(1 - m_d^*)\lambda^* + \frac{\kappa^*}{1 - X}\right] s^{*3} + (1 + \kappa^*\lambda^*)s^{*2} + (\lambda^* + \kappa^*)s^* + \kappa^*\lambda^* = 0 \qquad (91)$$

Since by definition $1 - m_d^* \geq 0$, $1 - X \geq 0$, and $\kappa^* \geq 0$, the coefficients of equation (91) are always positive. Therefore the boom system is always stable provided inequality (80) is satisfied. Substituting the appropriate value of the coefficients from equation (91) into inequality (80) yields

$$\frac{\kappa^{*3}\lambda^* X}{1 - X} - \kappa^{*2}\{m_d^* + \lambda^{*2}[m_d^* - (1 - m_d^*)X]\} - \kappa^*\lambda^*[m_d^*\lambda^{*2}(1 - m_d^*)(1 - X) + m_d^* - (1 - m_d^*)X] + (1 - m_d^*)\lambda^{*2}X < 0 \qquad (92)$$

provided $X \neq 1$

Equation (92) may be used to answer the following question. Given a fixed value of X and λ^*, what is minimum value of m_d^* (subsequently denoted by $m_{d_m}^*$) that will permit the boom to be stabilized? This is equivalent to finding the minimum value of m_d^* for which a real positive value of κ^* exists which satisfies equation (92). Corresponding values of $m_{d_m}^*$ and κ^* for various values of λ^* and X have been calculated on a digital computer. The results are shown in figures 9 and 10. At m_d^* equal to $m_{d_m}^*$

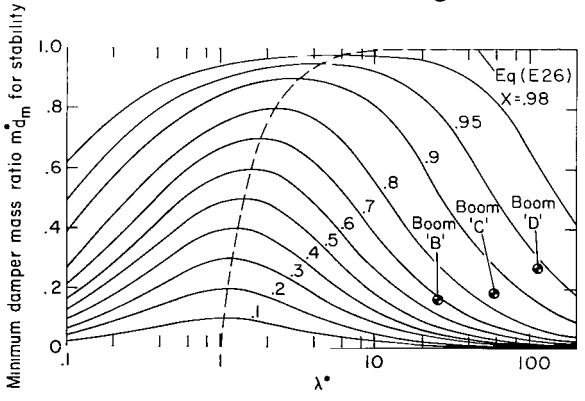

Figure 9.- Variation of minimum m_d^* for stability, with λ^*, for various values of X.

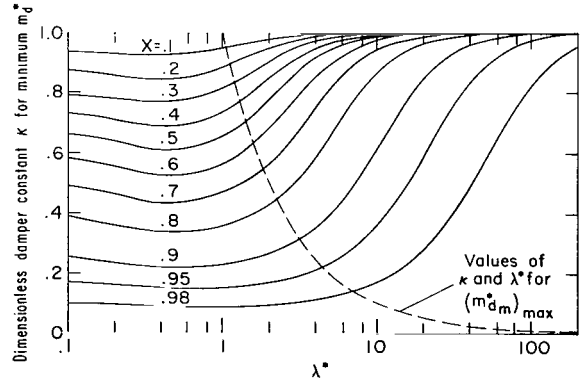

Figure 10.- Variation of κ for minimum m_d^*, with λ^*, for various values of X.

equation (92) has one real negative root and a pair of equal real positive roots. For values of m_d^* below the $m_{d_m}^*$ shown in figure 9, equation (92) has one real negative root and a pair of conjugate complex roots. In this case there is no real positive value of κ^* that satisfies equation (92) and therefore the boom cannot be stabilized. It is interesting that for a fixed value of X, there is a value of λ^* for which $m_{d_m}^*$ is a maximum. With this value of m_d^*, therefore, a boom with a given value of X can be stabilized irrespective of the material from which it is made. An analytical determination of the maximum value of $m_{d_m}^*$, for a given X, along with the value of λ^* at which it occurs, is given in appendix E. The results are summarized below

$$\left(m_{d_m}^*\right)_{max} = X \tag{93}$$

$$\lambda^* = \frac{1}{\sqrt{1 - X}} \tag{94}$$

$$\kappa^* = \sqrt{1 - X} \tag{95}$$

It is clear that, provided the value of X associated with a given boom is not too large, the damping scheme provides a practical solution. However, booms with open cross sections can have values of X close to unity and unless the value of λ^* is either very large or very small the technique may not offer a practical solution.

STABILITY OF TYPICAL OPEN SECTION BOOMS

The analytical results given in the previous sections show that there is a class of booms which can exhibit severe instabilities. In order to present the results in a compact form they are expressed in terms of dimensionless parameters. This method of presentation makes it difficult to visualize the physical dimensions and elastic properties of booms likely to experience instabilities. To provide data points relative to which other booms may be judged and to provide convincing evidence that existing boom systems can be unstable, the analytical results will be applied to specific examples. The pertinent parameters for these examples are given in the table. These parameters are typically those for silver plated copper-beryllium booms with a structurally open cross section. The thermal radiation constant is appropriate to a situation in which the sunline is normal to the boom axis. Both the radius of curvature and thermal time constant have been calculated assuming the boom cross section is thermally seamless (eqs. (4) and (5)). Boom A represents the OGO IV boom that is thought to have exhibited instability. Boom B is typical of one of the booms of a Naval Research Laboratory (NRL) gravity stabilized satellite which has experienced anomalous behavior. Boom C represents one of the booms of the Department of Defense Gravity Experiment

(DODGE) satellite which was observed by television camera but did not oscillate. Boom D represents one of the main booms of the ATS-D satellite.

The theory given in this report is based on the assumption that the mass of the boom is negligible compared with the mass of the tip. This is certainly not true for boom A. However, if it is assumed that the mode shape has only a secondary influence on stability then the boom mass can be represented as an equivalent tip mass. The magnitude of this tip mass is such that it gives the correct natural frequency of the first bending mode. Thus if the boom has no true tip mass, as is the case for boom A, then the natural fundamental frequency is $3.52\sqrt{EI/\sigma_m L^4}$ where σ_m is the mass per unit length of the boom. If Δm_T is the equivalent tip mass then

$$\sqrt{\frac{3EI}{\Delta m_T L^3}} = 3.52\sqrt{\frac{EI}{\sigma_m L^4}}$$

or

$$\Delta m_T = 0.242\ \sigma_m L \tag{96}$$

Similar considerations in torsion lead to an equivalent tip rotational inertia given by

$$\sqrt{\frac{C}{\Delta I_\psi}} = \frac{\pi}{2}\sqrt{\frac{C}{\sigma_I L^2}}$$

or

$$\Delta I_\psi = 0.406\ \sigma_I L \tag{97}$$

Equation (97) is only an approximation, since the effect of the warping stiffness has been ignored. However, the calculation is used only to demonstrate that inequality (38) is satisfied (see table) and, therefore, that rotational inertia effects on stability can be ignored. Equation (97) is sufficiently accurate for this purpose.

The values of λ^* and X for each of the example booms are plotted in figure 6. It is clear that boom A is the most unstable, having a value of $p^* \approx 0.14$. Therefore, in the absence of structural damping, boom A has an unstable oscillation which diverges as if it had a damping factor of -0.14.[1] The value of p^* for boom D is about half that for boom A. However, this fact does not give a balanced picture of the relative severity of the instabilities of these two booms. Thus, for example, the time to double the amplitude for boom A is only 0.46 minute while for boom D it is 17.20 minutes. This difference, of course, merely reflects the widely different frequencies of the two booms. However, it is important to note that in space applications the orientation of the run relative to the boom axis will generally vary with time as the satellite moves around its orbit. Therefore the conditions favorable to promoting instability in a given boom may occur for only part of the

[1]When C/EI is very small $\sqrt{m_T(A - B)} \approx \sqrt{m_T L^3/3EI}$ therefore $\zeta_z' \approx \zeta_z \approx -p^*$.

orbit. It follows that the greater the time to double the amplitude, the less will be the probability that its amplitude will be severe enough to influence the satellite or even be detectable. This may be the reason instabilities were never observed in boom C.

It follows from figure 7 that all the booms can be stabilized by flexural damping. In each case the required flexural damping factor is slightly higher than the corresponding value of $|p^*|$. On the other hand the values of λ^* for all the booms is considerably higher than 1.0, and it follows from figure 8 that none of the booms can be stabilized by torsional damping alone.

Although the booms can be stabilized by flexural damping the amount required for all the example booms is considerably higher than can be provided by the structure. The ball damper, however, seems to offer a practical solution to this problem for booms B, C, and D. In particular, boom D could be stabilized with a ball damper in which the ball is about 30 percent of the entire tip mass (see fig. 9). In fact a reasonable design approach would seem to be to assume that the boom has no structural damping and to size a ball damper to make the boom neutrally stable. The difficult question of deciding the exact value of the structural damping is thereby avoided.

CONCLUSIONS

A linearized dynamic stability analysis of slender booms, illuminated by thermal radiation and subject solely to self-induced thermal bending moments, leads to the following conclusions.

1. In the absence of structural damping any initially straight boom with either seamless or open cross section is unstable.

2. For most practical boom systems, including all that have been flown, the rotational inertia about the boom axis has a negligible effect on boom stability. Subsequent conclusions are all based on this simplification.

3. Initial curvature may increase or decrease the instability depending on its magnitude and direction. If the equilibrium shape of the boom, representing the combined effects of initial and thermally induced curvatures, is such that the boom and radiation source are on the same side of a plane passing through the boom root and perpendicular to the radiation rays, then the boom will be stable. In the absence of structural damping the converse is also true.

4. In the absence of structural damping, booms with a seamless cross section are only mildly unstable. They would probably be stabilized by their natural structural damping.

5. In the absence of structural damping, booms with open cross sections, characterized by a low ratio of torsional to bending stiffness, can be very unstable. Booms with an initial curvature may exhibit either oscillatory or

nonoscillatory instabilities depending on the magnitude and direction of the initial curvature. Initially straight booms, on the other hand, can only exhibit oscillatory instabilities. The worst case oscillatory instability has a frequency 66 percent of the natural flexural frequency and diverges as if it had a damping factor of -0.354. The magnitude of the instability is only slightly dependent on whether or not the cross section at the free end of the boom is restrained from warping. These booms can be stabilized by flexural damping but, in general, the amount required is greater than can be provided by the structure of existing booms.

6. Torsional damping is far less effective than flexural damping in suppressing the instability. There exists an important class of booms of open cross section which cannot be stabilized by torsional damping alone.

7. For a large class of booms, a passive ball type damper, attached to the tip of the booms seems to offer a practical solution to the problem of suppressing the instability.

Ames Research Center
National Aeronautics and Space Administration
Moffett Field, Calif., 94035, November 28, 1969

APPENDIX A

THERMAL BENDING MOMENTS IN A THERMALLY SEAMLESS THIN-WALL BOOM OF CIRCULAR SECTION HEATED BY THERMAL RADIATION

The primary aim of this appendix is to derive the linearized dynamic relationship between the thermal bending moment and the longitudinal twist of the boom.

First the normal modes and time constants of the temperature distribution are determined for a boom heated by parallel rays of thermal radiation. These modes are then used to obtain the steady-state temperature distribution around the boom cross section. Knowledge of the temperature distribution then permits the steady-state bending moments acting along the length of the boom to be calculated. It is then assumed that the boom is suddenly rotated about its axis through a small angle. The accompanying variation of temperature distribution, as expressed by the normal modes and time constants, is then used to determine the differential equation describing the variation of thermal bending moment with time. To simplify the analysis, assumptions similar to those used in reference 1 are made. These are given below for the sake of completeness.

1. The boom is sufficiently slender that heat conduction along its length may be neglected.

2. The entire cross section loses heat by radiation.

3. The radiant heat absorbed by an element on the sunlit side of the boom is proportional to the cosine of the angle between the surface normal at the element and the sun's rays.

4. Internal radiation is neglected.

The first of the above assumptions permits a reduction in the dimensionality of the heating problem since it implies that the thermal behavior of any section of the boom is independent of the thermal behavior of adjacent sections. Thus, the entire thermal behavior of the boom can be deduced when the behavior of a typical longitudinal section of small length is known.

TEMPERATURE DISTRIBUTION

The unsteady heat flow equations defining the temperature distribution around the circumference at a typical section along the boom and consistent with the above assumptions is

$$Kh \frac{\partial^2 \overline{T}(s,t')}{\partial s^2} - \rho ch \frac{\partial \overline{T}(s,t')}{\partial t'} = \sigma \varepsilon \overline{T}^4(s,t') - \gamma(s) \qquad (A1)$$

along with boundary conditions representing the fact that for a seamless circular cross section the temperature and its first derivative are continuous

$$\overline{T}(s,t') = \overline{T}(s + 2\pi r,t') \tag{A2}$$

$$\frac{\partial \overline{T}(s,t')}{\partial s} = \frac{\partial \overline{T}(s + 2\pi r,t')}{\partial s}$$

where

K	thermal conductivity
h	cylinder thickness
ρ	mass density
c	specific heat
σ	Stephan-Boltzmann constant
ϵ	emissivity
s	distance measured along the circumference
t'	time
$\overline{T}(s,t')$	absolute temperature at point s at time t'
r	cross-sectional radius
$\gamma(s)$	input heat flux rate due to thermal radiation

The analysis may be simplified further by making use of the observation that booms are usually made from materials whose thermal properties cause the temperature difference between any two points on the boom to be small compared with the absolute temperature of any point on the boom. Thus, if T_o is some average temperature and $T(s,t')$ is the difference between the temperature at the point s at time t' and the average temperature, then the ratio $T(s,t')/T_o$ is usually small. This permits use of the so-called linearizing assumption in which squares and higher orders of $T(s,t')/T_o$ are neglected.

By definition

$$\overline{T}(s,t') = T_o + T(s,t') \tag{A3}$$

and substituting for $\overline{T}(s,t')$ from equation (A3) into equations (A1) and (A2) and using the linearizing assumption gives the following equations for $T(s,t')$

$$\frac{\partial^2 T(s,t')}{\partial s^2} - \frac{\rho c}{K}\frac{\partial T(s,t')}{\partial t'} - \frac{4\sigma\epsilon T_o^3}{Kh}T(s,t') = -\frac{\gamma(s) + \sigma\epsilon T_o^4}{Kh} \tag{A4}$$

$$\left.\begin{aligned} T(s,t') &= T(s + 2\pi r, t') \\ \frac{\partial T(s,t')}{\partial s} &= \frac{\partial T(s + 2\pi r, t')}{\partial s} \end{aligned}\right\} \tag{A5}$$

The homogeneous part of equation (A4) is

$$\frac{\partial^2 T(s,t')}{\partial s^2} - \frac{\rho c}{K}\frac{\partial T(s,t')}{\partial t'} - \frac{4\sigma\epsilon T_o^3}{Kh}T(s,t') = 0 \tag{A6}$$

A solution to equation (A6) has the form

$$T(s,t') = e^{-\lambda t}A(s) \tag{A7}$$

where λ is a constant. Substituting for $T(s,t')$ from equation (A7) into equation (A6) gives the following ordinary differential equation for the function $A(s)$

$$\frac{d^2A(s)}{ds^2} - \Omega^2 A(s) = 0 \tag{A8}$$

where

$$\Omega^2 = \frac{4\sigma\epsilon T_o^3}{Kh} - \frac{\rho c\lambda}{K} \tag{A9}$$

The solution of equation (A8) is

$$A(s) = C_1 e^{\Omega s} + C_2 e^{-\Omega s} \tag{A10}$$

The value of Ω may now be found from the boundary conditions given by equations (A5). Substituting for $A(s)$ from equation (A10) into equation (A7) and for $T(s,t')$ from equation (A7) into equations (A5) gives

$$C_1 e^{\Omega s} + C_2 e^{-\Omega s} = C_1 e^{\Omega(s+2\pi r)} + C_2 e^{-\Omega(s+2\pi r)} \tag{A11}$$

$$C_1 e^{\Omega s} - C_2 e^{-\Omega s} = C_1 e^{\Omega(s+2\pi r)} - C_2 e^{-\Omega(s+2\pi r)} \tag{A12}$$

Equations (A11) and (A12) are satisfied for nontrivial values of C_1 and C_2 if and only if

$$\begin{vmatrix} \left(1 - e^{\Omega 2\pi r}\right) & \left(1 - e^{-\Omega 2\pi r}\right) \\ \left(1 - e^{\Omega 2\pi r}\right) & -\left(1 - e^{-\Omega 2\pi r}\right) \end{vmatrix} = 0$$

or

$$\left(1 - e^{\Omega 2\pi r}\right)\left(1 - e^{-\Omega 2\pi r}\right) = 0 \tag{A13}$$

Equation (A13) has a double root $e^{\Omega 2\pi r} = 1$ which, in turn, has roots given by

$$\Omega_n = \frac{in}{r} \qquad n = 0,1,2,\ldots \tag{A14}$$

where

$$i = \sqrt{-1}$$

The time constants λ_n can now be determined from equation (A9),

$$\lambda_n = \frac{4\sigma\varepsilon T_o^3}{h\rho c} + \frac{K}{\rho c}\left(\frac{n}{r}\right)^2 \tag{A15}$$

and the functions $A_n(s)$ from equation (A10),

$$A_n(s) = C_{1n}e^{in(s/r)} + C_{2n}e^{-in(s/r)}$$

which can be rewritten in the form

$$A_n(s) = A_{1n}(s) + A_{2n}(s) \tag{A16}$$

where

$$A_{1n}(s) = \left(C_{1n} + C_{2n}\right)\cos\frac{ns}{r}$$

$$A_{2n}(s) = i\left(C_{1n} - C_{2n}\right)\sin\frac{ns}{r}$$

The functions $A_{1n}(s)$ and $A_{2n}(s)$, $n = 0,1,2,\ldots$ are normal modes of the temperature distribution.

It now follows that the general solution of the homogeneous equation (A6) is

$$T(s,t') = \sum_{n=0}^{\infty} e^{\lambda_n t'}\left[A_{1n}(s) + A_{2n}(s)\right] \tag{A17}$$

Equation (A17) suggests a solution to the inhomogeneous equation (A4) of the form

$$T(s,t') = \sum_{n=0}^{\infty}\left[q_{1n}(t')\cos\frac{ns}{r} + q_{2n}(t')\sin\frac{ns}{r}\right] \tag{A18}$$

where the constants $C_{1n} + C_{2n}$ and $i(C_{1n} - C_{2n})$ are included in the functions $q_{1n}(t')$ and $q_{2n}(t')$, respectively. Substituting equation (A18) into equation (A4) and using equations (A8) and (A9) yields the equation

$$\sum_{n=0}^{\infty}\left\{\left[\frac{dq_{1n}(t')}{dt'} + \lambda_n q_n(t')\right]\cos\frac{ns}{r} + \left[\frac{dq_{2n}(t')}{dt'} + \lambda_n q_{2n}(t')\right]\right\} = \frac{\gamma(s)-\sigma\varepsilon T_o^4}{h\rho c} \tag{A19}$$

which must be satisfied by $q_{1n}(t')$ and $q_{2n}(t')$ for equation (A18) to be a solution.

STEADY-STATE BENDING MOMENTS

Consider now the situation as shown in figure 11(a), where the y'' and z'' axes are assumed to be fixed in the cross section. By assumption 3 the input

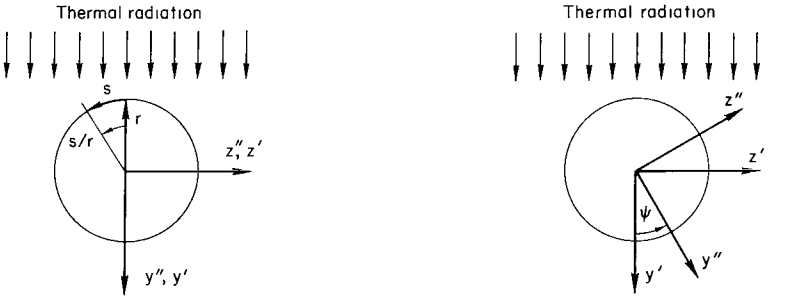

(a) Before rotation. (b) After rotation ψ.

Figure 11.- Coordinate systems for thermal analysis.

heat flux rate due to solar radiation is given by the expression

$$\gamma(s) = J_s\alpha_s\Theta(s)\cos\frac{s}{r} \tag{A20}$$

where

J_s = thermal radiation constant

α_s = absorptivity

and

$$\Theta(s) = 1 \quad \text{for} \quad \cos\frac{s}{r} \geq 0$$

$$= 0 \quad \text{for} \quad \cos\frac{s}{r} < 0$$

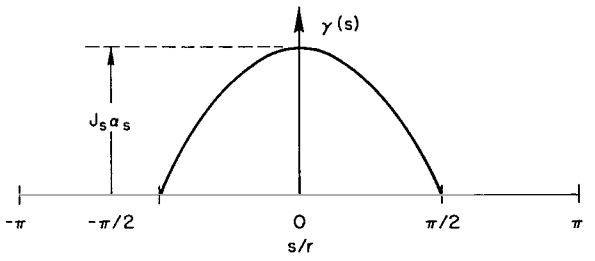

Figure 12.- Circumferential distribution of input heat flux rate.

The variation of $\gamma(s)$ with s/r is shown in figure 12. It follows from equation (A20) that $\gamma(s)$ is an even function of s/r. Therefore, since $\sigma\epsilon T_o^4$ is a constant, the left hand side of equation (A19) is also an even function of s/r. Since the left hand side of equation (A19) is a Fourier series with argument s/r, it follows that equation (A19) can be satisfied if and only if $q_{2n}(t') \equiv 0$ for all n.

It is shown in reference 1 (after sign adjustments to account for the adopted axis system) that the thermally induced bending moments about the y'' and z'' axes are given by the expressions

$$M_{y''}(t') = e_c E h \int_0^{2\pi r} T(s,t') z''(s) ds \tag{A21}$$

$$M_{z''}(t') = -e_c E h \int_0^{2\pi r} T(s,t') y''(s) ds \tag{A22}$$

where

e_c coefficient of thermal expansion

E Young's modulus

$\left.\begin{matrix} y''(s) \\ z''(s) \end{matrix}\right\}$ y'' and z'' coordinates of a point s on the perimeter of the boom

It follows from figure 11 that

$$y''(s) = -r \cos \frac{s}{r} \tag{A23}$$

$$z''(s) = -r \sin \frac{s}{r} \tag{A24}$$

Substituting equation (A18) into equations (A21) and (A22) (noting that $q_{2n}(t') \equiv 0$ for all n) and performing the integrations indicated gives the following expressions

$$M_{y''}(t') = 0 \tag{A25}$$

$$M_{z''}(t') = e_c E h \pi r^2 q_{11}(t') \tag{A26}$$

However, it follows from equation (A19) that $[dq_{11}(t')/dt'] + \lambda_1 q_{11}(t')$ is equal to the coefficient of $\cos(s/r)$ in the Fourier expansion of $\gamma(s) - \sigma\varepsilon T_o^4/h\rho c$. Thus,

$$\frac{dq_{11}(t')}{dt'} + \lambda_1 q_{11}(t') = \frac{J_s \alpha_s}{2h\rho c} \tag{A27}$$

Equations (A26) and (A27) may now be combined to give the following expression for $M_{z''}(t')$ in terms of the material properties. Thus,

$$\frac{dM_{z''}(t')}{dt'} + \lambda_1 M_{z''}(t') = \frac{J_s \alpha_s e_c E \pi r^2}{2\rho c} \tag{A28}$$

Equations (A25) and (A28) show that in the steady state,

$$\begin{aligned} M_{y''}(\infty) &= 0 \\ M_{z''}(\infty) &= \frac{J_s \alpha_s e_c E \pi r^2}{2\rho c \lambda_1} \end{aligned} \tag{A29}$$

CHANGE OF BENDING MOMENTS DUE TO SMALL ROTATION

Suppose, now, that the boom, whose cross section is shown in figure 11, has reached its steady-state temperature distribution. The bending moments acting on the boom are given by equation (A29). Suppose, further, that the cross section is instantaneously rotated through a small angle ψ. It is required to know the equations defining the subsequent change in the thermal bending moments.

The equation governing the perturbation in temperature caused by the small rotation differs from equation (A4) only in that the right hand side is replaced by $-\Delta\gamma(s)/Kh$ where $\Delta\gamma(s)$ is the change of heat flux rate. It should be noted here that t is the time measured from the instant of rotation through the angle ψ. The equation corresponding to equation (A19) is, therefore

$$\sum_{n=0}^{\infty} \left\{ \left[\frac{d\Delta q_{1n}(t)}{dt} + \lambda_n \Delta q_{1n}(t) \right] \cos \frac{ns}{r} + \left[\frac{d\Delta q_{2n}(t)}{dt} + \lambda_n \Delta q_{2n}(t) \right] \sin \frac{ns}{r} \right\} = \frac{\Delta\gamma(s)}{h\rho c} \tag{A30}$$

The instantaneous change of heat flux rate is given by (see eq. (A20))

$$\Delta\gamma(s) = J_s \alpha_s \left[\theta_1(s) \cos\left(\frac{s}{r} + \psi\right) - \theta_2(s) \cos \frac{s}{r} \right] \tag{A31}$$

where

$$\begin{aligned} \theta_1(s) &= 1 \qquad \cos\left(\frac{s}{r} + \psi\right) \geq 0 \\ &= 0 \qquad \cos\left(\frac{s}{r} + \psi\right) < 0 \end{aligned}$$

$$\Theta_2(s) = 1 \qquad \cos\frac{s}{r} \geq 0$$

$$= 0 \qquad \cos\frac{s}{r} < 0$$

If ψ is assumed to be sufficiently small that only terms linear in ψ need be retained, equation (A31) becomes

$$\Delta\gamma(s) = -J_s\alpha_s\Theta(s)\psi \sin\frac{s}{r} \tag{A32}$$

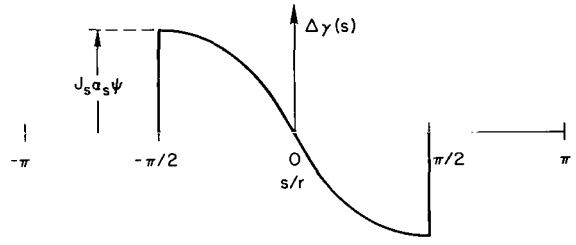

Figure 13.- Change of circumferential distribution of input heat flux rate due to twist.

The variation of $\Delta\gamma(s)$ with s/r is shown in figure 13. Clearly, $\Delta\gamma(s)$ is an odd function of s/r; therefore, equation (A30) shows that $\Delta q_{1n}(t) \equiv 0$ for all n.

Proceeding as for equations (A25) and (A26) gives corresponding expressions for the changes in the thermal bending moments; thus,

$$\Delta M_{y''}(t) = -e_c E h \pi r^2 \Delta q_{21}(t) \tag{A33}$$

$$\Delta M_{z''}(t) = 0$$

Equation (A30) shows that the expression $[d\Delta q_{21}(t)/dt] + \lambda_1\Delta q_{21}(t)$ is equal to the coefficient of $\sin(s/r)$ in the Fourier expansion of $\Delta\gamma(s)/h\rho c$. Thus,

$$\frac{d\Delta q_{21}(t)}{dt} + \lambda_1\Delta q_{21}(t) = -\frac{J_s\alpha_s\psi}{2h\rho c} \tag{A34}$$

Equations (A33) and (A34) may now be combined to give the following expressions for $\Delta M_{y''}(t)$

$$\frac{d\Delta M_{y''}(t)}{dt} + \lambda_1\Delta M_{y''}(t) = \frac{J_s\alpha_s e_c E\pi r^2\psi}{2\rho c} \tag{A35}$$

Equation (A35) may now be combined with equation (A29) to yield

$$\frac{d\Delta M_{y''}(t)}{dt} + \lambda_1\Delta M_{y''}(t) = \lambda_1 M_{z''}(\infty)\psi \tag{A36}$$

The bending moment $\Delta M_{y''}(t)$ may now be resolved about a set of axes y' and z' (see fig. 11(b)) which are fixed relative to the direction of the incident radiation. The component $\Delta M_{y'}(t)$ about the y' axis is given by $\Delta M_{y''}(t)\cos\psi \approx \Delta M_{y'}(t)$ while the component $\Delta M_{z'}(t)$ about the z' axis is given by $\Delta M_{y''}(t)\sin\psi \approx 0$ (since by eq. (A36) $\Delta M_{y'}(t)$ is the same order as ψ). The overall conclusion, therefore, is that following an instantaneous rotation ψ, the thermal bending moments acting on the cross section consist of

(a) A moment $M_{z''}(\infty)$ whose direction rotates with the cross section (body fixed moment) and whose magnitude is constant and given by equation (A29)

(b) A moment $\Delta M_{y'}(t)$ whose direction is along the rays of the incident radiation and whose magnitude is given by

$$\frac{d\Delta M_{y'}(t)}{dt} + \lambda_1 \Delta M_{y'}(t) = \lambda_1 M_{z''}(\infty)\psi(t) \tag{A37}$$

where $\psi(t)$ is regarded as a function of time.

APPENDIX B

DEFLECTION EQUATIONS FOR A CIRCULARLY BENT BOOM OF CIRCULAR CROSS SECTION

Consider a boom whose locus of flexural centers, in the unloaded condition, forms the arc of a circle of radius R. Furthermore, let the boom be attached rigidly at one end to form a cantilever. It is assumed from the outset that the length of the boom L is small compared with the radius of curvature R. The situation is shown in figure 14 which also shows the coordinate systems adopted. The unit vectors $\bar{t}(x)$, $\bar{n}(x)$, and $\bar{b}(x)$ at a typical point A are the tangent, normal, and binormal, respectively, to the locus of flexural centers. The coordinates of point A relative to the $\bar{t}(0)$, $\bar{n}(0)$, $\bar{b}(0)$ axes are x_o, y_o, z_o while the deflection of point A relative to the $\bar{n}(x)$, $\bar{b}(x)$ axes are denoted by $y(x)$ and $z(x)$. The angle of twist about $\bar{t}(x)$ is denoted by $\psi(x)$.

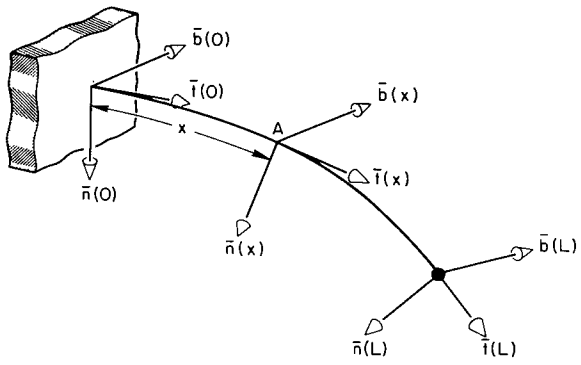

Figure 14.- Coordinate system for deflection analysis.

The problem is to determine the tip deflections $y(L)$ and $z(L)$ and the twist $\psi(L)$ due to the simultaneous action of forces F_y and F_z acting along $\bar{n}(L)$ and $\bar{b}(L)$, a couple T acting along $\bar{t}(L)$ and an arbitrary distribution of bending moments $\Delta M_n(x)$ and $\Delta M_b(x)$ acting along $\bar{n}(x)$ and $\bar{b}(x)$. The loads on the boom are shown in figure 15. The assumption is now made that the boom deflections are sufficiently small that the principal of superposition holds and that, therefore, the bending moments and torques remain constant and equal to their values calculated as if the boom were undeflected. It follows from figure 15 that the total bending moments $M_n(x)$ and $M_b(x)$ along $\bar{n}(x)$ and $\bar{b}(x)$, respectively, at point A, are

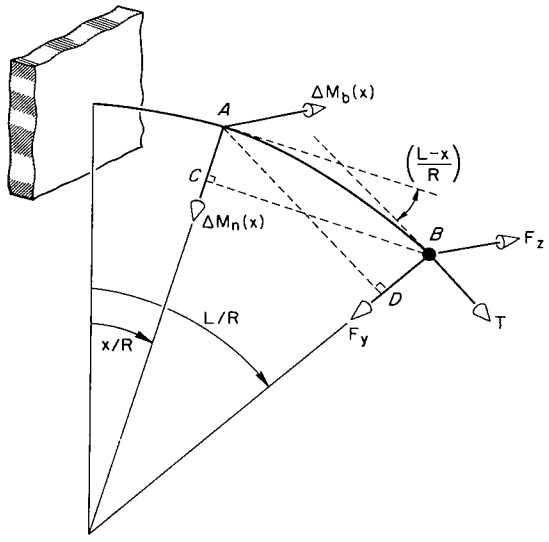

Figure 15.- Loads acting on the boom.

$$M_n(x) = -F_z \overline{BC} + T \sin\left(\frac{L - x}{R}\right) + \Delta M_n(x)$$

$$M_b(x) = F_y \overline{AD} + \Delta M_b(x)$$

while the torque $M_t(x)$ along $\bar{t}(x)$ is given by

$$M_t(x) = F_z \overline{AC} + T \cos \frac{L - x}{R}$$

The distances $\overline{BC}$, $\overline{AD}$, and $\overline{AC}$ are given by the following expressions

$$\overline{BC} = \overline{AD} = R \sin \frac{L - x}{R}$$

$$\overline{AC} = R\left(1 - \cos \frac{L - x}{R}\right)$$

It is assumed at this point that the order of magnitude of the ratio of the couple T to either force F_z or F_y never exceeds L^2/R. Expanding the above expressions into powers of $(L - x)/R$ and neglecting all above the third power in the moments due to F_y and F_z and the first power in moments due to T (in agreement with the above assumption) yields the following expressions for $M_n(x)$, $M_b(x)$, and $M_t(x)$

$$M_n(x) = -F_z\left[(L - x) - \frac{(L - x)^3}{6R^2}\right] + \frac{T}{R}(L - x) + \Delta M_n(x) \tag{B1}$$

$$M_b(x) = F_y\left[(L - x) - \frac{(L - x)^3}{6R^2}\right] + \Delta M_b(x) \tag{B2}$$

$$M_t(x) = F_x \frac{(L - x)^2}{2R} + T \tag{B3}$$

It is convenient to start with the calculation of $\psi(x)$. The twist angle of a bent boom can be regarded as the sum of two components, one representing the contribution due to twisting torque, the other the contribution due to bending. Thus,

$$\psi(x) = \psi_T(x) + \psi_B(x) \tag{B4}$$

The relationship between angle of twist and applied torque is given by the differential equation (ref. 6)

$$-C_1 \frac{d^3\psi_T(x)}{dx^3} + C \frac{d\psi_T(x)}{dx} = M_t(x) \tag{B5}$$

The appropriate solution of equation (B5) must satisfy the following end conditions

$$\psi_T(x)\Big|_{x=0} = 0 \tag{B6}$$

$$\left.\frac{d\psi_T(x)}{dx}\right|_{x=0} = 0 \tag{B7}$$

along with

$$\left.\frac{d\psi_T(x)}{dx}\right|_{x=L} = 0 \quad \text{if Tip Warping is Restrained (TWR)} \tag{B8}$$

or

$$\left.\frac{d^2\psi_T(x)}{dx^2}\right|_{x=L} = 0 \quad \text{if Tip Warping is Unrestrained (TWU)} \tag{B9}$$

The appropriate solution of equation (B5) is given by

$$\psi_T(x) = \int_0^x \left\{ \beta \sinh(k\bar{x}) - \frac{1}{C_1 k} \int_0^{\bar{x}} M_t(\hat{x}) \sinh[k(\bar{x} - \hat{x})]\, d\hat{x} \right\} d\bar{x} \tag{B10}$$

where

$$k = \sqrt{\frac{C}{C_1}}$$

$$\beta = \frac{1}{C_1 k \sinh(kL)} \int_0^L M_t(\hat{x}) \sinh[k(L - \hat{x})]\, d\hat{x} \quad \text{(TWR)} \tag{B11}$$

or

$$\beta = \frac{1}{C_1 k \cosh(kL)} \int_0^L M_t(\hat{x}) \cosh[k(L - \hat{x})]\, d\hat{x} \quad \text{(TWU)} \tag{B12}$$

Substituting equation (B3) into equations (B10), (B11), and (B12) and performing the integrations gives the following results

$$\psi_T(x) = \frac{F_z}{6RC} \left(x^3 + 3Lx(L - x) + \frac{6x}{k^2} + \frac{3[(kL)^2 + 2]}{k^3 \sinh(kL)} \{\cosh[k(L - x)] - \cosh(kL)\} \right.$$

$$\left. + \frac{6[1 - \cosh(kx)]}{k^3 \sinh(kL)} \right) + \frac{T}{C} \left\{ x - \frac{\cosh(kx) - \cosh[k(L - x)]}{k \sinh(kL)} - \frac{\tanh\left(\frac{kL}{2}\right)}{k} \right\} \quad \text{(TWR)} \tag{B13}$$

or

$$\psi_T(x) = \frac{F_z}{6RC}\left(x^3 + 3Lx(L-x) + \frac{6x}{k^2} + \frac{3[(kL)^2+2]}{k^3\cosh(kL)}\{\sinh[k(L-x)] - \sinh(kL)\}\right)$$

$$+ \frac{T}{C}\left\{x + \frac{\sinh[k(L-x)]}{k\cosh(kL)} - \frac{\tanh(kL)}{k}\right\} \qquad \text{(TWU)} \qquad \text{(B14)}$$

When $x = L$

$$\psi_T(L) = \frac{F_z L^3 f_1(kL)}{6RC} + \frac{TLf_2(kL)}{C} \qquad \text{(B15)}$$

where

$$\left.\begin{aligned} f_1(kL) &= 1 + \frac{6}{(kL)^2} - \frac{3[(kL)^2+4]}{(kL)^3}\tanh\left(\frac{kL}{2}\right) \\ f_2(kL) &= 1 - \frac{2}{kL}\tanh\left(\frac{kL}{2}\right) \end{aligned}\right\} \text{TWR}$$

or

$$\left.\begin{aligned} f_1(kL) &= 1 + \frac{6}{(kL)^2} - \frac{3[(kL)^2+2]}{(kL)^3}\tanh(kL) \\ f_2(kL) &= 1 - \frac{1}{kL}\tanh(kL) \end{aligned}\right\} \text{TWU} \qquad \text{(B16)}$$

Graphs of $f_1(kL)$ and $f_2(kL)$ are given in figure 3.

The twist due to bending $\psi_B(x)$ may be obtained from the strain energy due to bending by application of Castigliano's theorem (ref. 7). It is first necessary to introduce, in addition to the loads indicated in figure 15, a dummy torque T_t acting at the point x and along the tangent to the boom axis. The bending moment at the point $\hat{x}$ about the $n(\hat{x})$ axis then becomes

$$\left.\begin{aligned} M_n'(\hat{x}) &= M_n(\hat{x}) + T_t \sin\left(\frac{x-\hat{x}}{R}\right) && x \geq \hat{x} \\ &= M_n(\hat{x}) && x < \hat{x} \end{aligned}\right\} \qquad \text{(B17)}$$

while the bending moment about the $\bar{b}(\hat{x})$ axis remains unchanged. The strain energy in bending is given by the expression

$$U_B = \int_0^L \left\{\frac{[M_n'(\hat{x})]^2}{2EI} + \frac{[M_b(\hat{x})]^2}{2EI}\right\} d\hat{x} \qquad \text{(B18)}$$

and by the Castigliano theorem

$$\psi_B(x) = \left(\frac{\partial U_B}{\partial T_t}\right)_{T_t=0} = \int_0^L \frac{M_n(\hat{x})}{EI} \frac{\partial [M_n'(\hat{x})]}{\partial T_t} d\hat{x} \tag{B19}$$

Differentiating equation (B17) with respect to T_t and substituting for $\partial[M_n'(\hat{x})]/\partial T_t$ in equation (B19) yields

$$\psi_B(x) = \frac{1}{EI} \int_0^x M_n(\hat{x}) \sin\left(\frac{x - \hat{x}}{R}\right) d\hat{x} \tag{B20}$$

Substituting for $M_n(\hat{x})$ from equation (B1) into equation (B20) and performing the integration indicated yields the following expression for $\psi_B(x)$

$$\psi_B(x) = \frac{-F_z}{EIR}\left(\frac{Lx^2}{2} - \frac{x^3}{6}\right) + \frac{1}{EI} \int_0^x \Delta M_n(\hat{x}) \sin\left(\frac{x - \hat{x}}{R}\right) d\hat{x} \tag{B21}$$

where the simplifications permitted by the assumption made about the relative magnitudes of the forces F_y and F_z to the torque T have been made and terms of order $F_z L^5/R^3$ and higher have been neglected.

Combining equations (B15) and (B21) yields

$$\psi(L) = \frac{F_z L^3}{3R}\left[\frac{f_1(kL)}{2C} - \frac{1}{EI}\right] + \frac{TLf_2(kL)}{C} + \frac{1}{EI} \int_0^L \Delta M_n(\hat{x}) \sin\left(\frac{L - \hat{x}}{R}\right) d\hat{x} \tag{B22}$$

The linear deflections $y(L)$ and $z(L)$ may also be regarded as the sum of two components. In this case they are the contributions due to the bending moment and to the angle of twist $\psi_T(x)$

$$\left.\begin{aligned} y(L) &= y_B(L) + y_T(L) \\ z(L) &= z_B(L) + z_T(L) \end{aligned}\right\} \tag{B23}$$

The contributions $y_B(L)$ and $z_B(L)$ may be calculated from the strain energy in bending by an application of Castigliano's theorem. Thus the stain energy in bending is given by equation (B18) where in this case the dummy torque T_t need not be included. The expressions for $y_B(L)$ and $z_B(L)$, by Castigliano, are

$$y_B(L) = \frac{\partial U_B}{\partial F_y} = \frac{1}{EI} \int_0^L M_b(x) \frac{\partial M_b(x)}{\partial F_y} dx \tag{B24}$$

$$z_B(L) = \frac{\partial U_B}{\partial F_z} = \frac{1}{EI} \int_0^L M_n(x) \frac{\partial M_n(x)}{\partial F_z} dx \tag{B25}$$

where use has been made of the facts that, from equations (B1) and (B2), $\partial M_n(x)/\partial F_y = \partial M_b(x)/\partial F_z = 0$. Substituting from equations (B1) and (B2) into equations (B24) and (B25) yields

$$y_B(L) = \frac{F_y}{EI} \int_0^L \left[(L - x) - \frac{(L - x)^3}{6R^2}\right]^2 dx + \frac{R}{EI} \int_0^L \Delta M_b(x) \sin\left(\frac{L - x}{R}\right) dx \tag{B26}$$

$$z_B(L) = \frac{F_z}{EI} \int_0^L \left[(L - x) - \frac{(L - x)^3}{6R^2}\right]^2 dx - \frac{T}{REI} \int_0^L (L - x) \left[(L - x) - \frac{(L - x)^3}{6R^2}\right] dx$$

$$- \frac{R}{EI} \int_0^L \Delta M_n(x) \sin\left(\frac{L - x}{R}\right) dx \tag{B27}$$

where the quantity $(L - x) - [(L - x)^3/6R^2]$, which is an approximation to $R \sin[(L - x)/R]$, has been replaced by its true value in the two integral expressions. Equations (B26) and (B27) simplify to

$$y_B(L) = \frac{F_y}{3EI}\left(L^3 - \frac{L^5}{5R^2}\right) + \frac{R}{EI} \int_0^L \Delta M_b(x) \sin\left(\frac{L - x}{R}\right) dx \tag{B28}$$

$$z_B(L) = \frac{F_z}{3EI}\left(L^3 - \frac{L^5}{5R^2}\right) - \frac{TL^3}{3REI} - \frac{R}{EI} \int_0^L \Delta M_n(x) \sin\left(\frac{L - x}{R}\right) dx \tag{B29}$$

It follows from the geometry of the boom in the deflected state that, to the required accuracy, the deflection $y_T(L)$, due to twist, is zero, while the deflection $z_T(L)$ is given by the expression

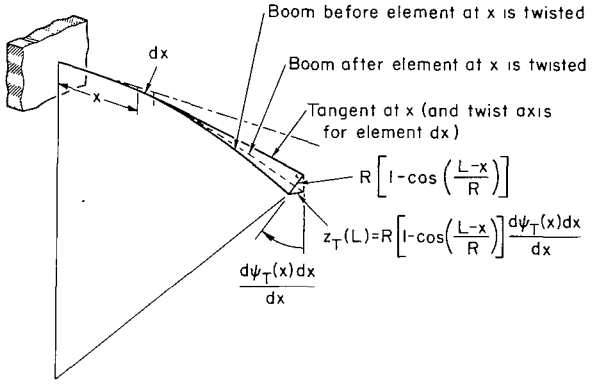

Figure 16.- Geometry of the linear deflection due to twist.

$$z_T(L) = R \int_0^L \left[1 - \cos\left(\frac{L - x}{R}\right)\right] \frac{d\psi_T(x)}{dx} dx \tag{B30}$$

(see fig. 16)

Integrating equation (B30) by parts gives

$$z_T(L) = \int_0^L \psi_T(x) \sin\left(\frac{L - x}{R}\right) dx \tag{B31}$$

Substituting for $\psi_T(x)$ from equations (B15) and (B16) into equation (B31) and approximating $\sin[(L - x)/R]$ by

(L - x)/R yields

$$z_T(L) = \frac{F_z L^5 f_3(kL)}{20R^2C} + \frac{TL^3 f_1(kL)}{6RC} \tag{B32}$$

where

$$f_3(kL) = 1 + \frac{40}{3(kL)^2} + \frac{20}{(kL)^4} - \frac{5}{(kL)^5}\left\{4[(kL)^2 + 2]\tanh\left(\frac{kL}{2}\right) + (kL)^4 \coth(kL)\right\} \quad \text{TWR}$$

or

$$f_3(kL) = 1 + \frac{40}{3(kL)^2} + \frac{20}{(kL)^4} - \frac{5[(kL)^2 + 2]^2}{(kL)^5}\tanh(kL) \quad \text{TWU}$$

(B33)

Graphs of $f_3(kL)$ are given in figure 3.

It follows from equations (B28), (B29), and (B32) that

$$y(L) = \frac{F_y}{3EI}\left(L^3 - \frac{L^5}{5R^2}\right) + \frac{R}{EI}\int_0^L \Delta M_b(x)\sin\left(\frac{L - x}{R}\right) dx \tag{B34}$$

$$z(L) = F_z\left\{\frac{L^3}{3EI} + \frac{L^5}{5R^2}\left[\frac{f_3(kL)}{4C} - \frac{1}{3EI}\right]\right\} + \frac{TL^3}{3R}\left[\frac{f_1(kL)}{2C} - \frac{1}{EI}\right] - \frac{R}{EI}\int_0^L \Delta M_n(x)\sin\left(\frac{L - x}{R}\right) dx \tag{B35}$$

APPENDIX C

ORDER OF MAGNITUDE OF ANGLE OF TWIST DUE TO THERMAL BENDING MOMENTS

At any point x along the boom, the angle of twist due to thermal bending moments is given by the expression $[N(x,t)/RR_S]\sin\alpha$, where

$$N(x,t) = R\int_0^x \eta(\hat{x},t)\sin\left(\frac{x-\hat{x}}{R}\right)d\hat{x} \tag{C1}$$

These two expressions follow from equations (12) and (13) with L replaced by x. The quantity $\eta(\hat{x},t)$ is given by equation (6), which has the general solution

$$\eta(\hat{x},t) = e^{-\lambda t}\eta(\hat{x},0) + \lambda\int_0^t e^{-\lambda(t-\tau)}\psi(\hat{x},\tau)d\tau \tag{C2}$$

Since, by definition, the boom is undisturbed at $t = 0$ it follows that $\eta(\hat{x},0) = 0$. Also $\psi(\hat{x},\tau)$ is continuous in τ and $e^{-\lambda(t-\tau)}$ is positive and integrable over the region $0 \le \tau \le t$. Therefore the first integral theorem of mean value may be applied to equation (C2) giving

$$\eta(\hat{x},t) = \lambda\psi(\hat{x},\overline{\tau})\int_0^t e^{-\lambda(t-\tau)}d\tau \tag{C3}$$

where $0 \le \overline{\tau} \le t$. Therefore

$$\eta(\hat{x},t) = \psi(\hat{x},\overline{\tau})\left(1 - e^{-\lambda t}\right) \tag{C4}$$

Since $\eta(\hat{x},t)$ is continuous and $(x - \hat{x})$ is positive and integrable over the interval $0 \le \hat{x} \le x$, the first integral of mean value may be applied to equation (C1) giving

$$N(x,t) = R\eta(\overline{x},t)\int_0^x \sin\left(\frac{x-\hat{x}}{R}\right)d\hat{x}$$

where $0 \le \overline{x} \le x$. Therefore,

$$N(x,t) = R\eta(\overline{x},t)\left(1 - \cos\frac{x}{R}\right) \tag{C5}$$

It follows from equations (C4) and (C5) that

$$N(x,t) = R\psi(\bar{x},\bar{\tau})\left(1 - \cos\frac{x}{R}\right)\left(1 - e^{-\lambda t}\right)$$

or

$$N(x,t) < R\psi(\bar{x},\bar{\tau})\left(1 - \cos\frac{x}{R}\right) \qquad (t > 0) \tag{C6}$$

If it is assumed that $\psi(x,\bar{\tau}) > \psi(\bar{x},\bar{\tau})$, inequality (C6) can be expressed in the form

$$\frac{N(x,t)}{RR_s}\sin\alpha < \psi(x,\bar{\tau})\,\frac{x^2\sin\alpha}{2RR_s} \qquad (t > 0) \tag{C7}$$

where the factor $[1 - \cos(x/R)]$ has been replaced by its approximate value $x^2/2R^2$. Inequality (C7) indicates that over any interval of time starting at zero the maximum angle of twist due to thermal bending moments alone is less than the maximum total angle of twist multiplied by the factor $(x^2/2RR_s)\sin\alpha$.

APPENDIX D

EVALUATION OF THE REAL PART OF THE ROOT OF THE STABILITY POLYNOMIAL CORRESPONDING TO THE MOST RAPID DIVERGENCE

The stability polynomial for the special case of $I_\psi = D_\psi = 0$ is (eq. (51))

$$\frac{s^{*3}}{1 - X} + \left(\frac{2\zeta_z}{1 - X} + \lambda^*\right)s^{*2} + (1 + 2\lambda^*\zeta_z)s^* + \lambda^* = 0 \tag{D1}$$

where the variables are defined by equations (47) to (50). In this appendix the real part of the root of equation (D1) corresponding to the most rapid divergence is sought under conditions of (a) varying λ^* at a fixed X, and (b) varying X at a fixed λ^*.

It follows from the stability criteria for a cubic given in reference 5 that the unstable mode, if it exists, must be oscillatory. It is therefore assumed that, in the region of interest, equation (D1) has one real root and a pair of conjugate imaginary roots. Thus the characteristic polynomial must have the following representation

$$(s^* + a^*)(s^{*2} - 2p^*s^* + p^{*2} + q^{*2}) = 0 \tag{D2}$$

where p^* is the real part of the most rapid divergence and a^* and q^* are both real quantities. Equation (D2) may be expanded to give

$$s^{*3} + s^{*2}(-2p^* + a^*) + s(p^{*2} + q^{*2} - 2p^*a^*) + a^*(p^{*2} + q^{*2}) = 0 \tag{D3}$$

Equating coefficients of equations (D1) and (D3)

$$-2p^* + a^* = 2\zeta_z + \lambda^*(1 - X) \tag{D4}$$

$$p^{*2} + q^{*2} - 2p^*a^* = (1 - X)(1 + 2\lambda^*\zeta_z) \tag{D5}$$

$$a^*(p^{*2} + q^{*2}) = \lambda^*(1 - X) \tag{D6}$$

VARYING λ^*, FIXED X

At a stationary value of p^* with respect to λ^* it is necessary that $\partial p^*/\partial \lambda^* = 0$. The result of differentiating equations (D4), (D5), and (D6)

with respect to λ^* is

$$\frac{\partial a^*}{\partial \lambda^*} = 1 - X \tag{D7}$$

$$2q^* \frac{\partial q^*}{\partial \lambda^*} - 2p^* \frac{\partial a^*}{\partial \lambda^*} = 2\zeta_z(1 - X) \tag{D8}$$

$$\frac{\partial a^*}{\partial \lambda^*} (p^{*2} + q^{*2}) + 2a^*q^* \frac{\partial q^*}{\partial \lambda^*} = (1 - X) \tag{D9}$$

Equations (D7), (D8), and (D9) hold for nontrivial values of $\partial a^*/\partial \lambda^*$ and $q^*(\partial q^*/\partial \lambda^*)$ if and only if

$$\begin{vmatrix} 1 & 0 & -(1 - X) \\ -2p^* & 2 & -2\zeta_z(1 - X) \\ p^{*2} + q^{*2} & 2a^* & -(1 - X) \end{vmatrix} = 0 \tag{D10}$$

If $x \neq 1$, equation (D10) simplifies to

$$p^{*2} + q^{*2} + 2a^*p^* + 2a^*\zeta_z = 1 \tag{D11}$$

It also follows from equations (D4) and (D6), after eliminating $\lambda^*(1 - X)$, that

$$a^*(p^{*2} + q^{*2}) = -2p^* + a^* - 2\zeta_z \tag{D12}$$

and from equations (D11) and (D12) by eliminating $p^{*2} + q^{*2}$ that

$$a^{*2} = 1 \tag{D13}$$

Since p^* and q^* are real by definition, equation (D6) shows that a^* must be positive for $X < 1$. Therefore

$$a^* = 1 \tag{D14}$$

Equations (D5), (D6), and (D14) may be combined to eliminate λ^*, yielding

$$p^{*2} + q^{*2} - 2p^* = 2\zeta_z(p^{*2} + q^{*2}) + 1 - X \tag{D15}$$

Eliminating $p^{*2} + q^{*2}$ between equations (D11) and (D15) gives the following expression for p^*

$$p^* = \frac{X}{4(1 - \zeta_z)} - \zeta_z \tag{D16}$$

Substituting for p^* from equation (D16) into equation (D4) produces the following equation for λ^*

$$\lambda^* = \frac{1}{1 - X}\left[1 - \frac{X}{2(1 - \zeta_z)}\right] \tag{D17}$$

The imaginary part of the complex root may be obtained from equation (D11); thus,

$$q^{*2} = 1 - p^{*2} - 2(p^* + \zeta_z) \tag{D18}$$

VARYING X, FIXED λ^*

At a stationary value of p^* with respect to X it is necessary that $\partial p^*/\partial X = 0$. The result of differentiating equations (D4), (D5), and (D6) with respect to X is

$$\frac{\partial a^*}{\partial X} = -\lambda^* \tag{D19}$$

$$2q^* \frac{\partial q^*}{\partial X} - 2p^* \frac{\partial a^*}{\partial X} = -(1 + 2\lambda^*\zeta_z) \tag{D20}$$

$$\frac{\partial a^*}{\partial X}(p^{*2} + q^{*2}) + 2a^*q^* \frac{\partial q^*}{\partial X} = -\lambda^* \tag{D21}$$

Equations (D19), (D20), and (D21) hold for nontrivial values of $\partial a^*/\partial X$ and $q^*(\partial q^*/\partial X)$ if and only if

$$\begin{vmatrix} 1 & 0 & \lambda^* \\ -2p^* & 2 & 1 + 2\lambda^*\zeta_z \\ p^{*2} + q^{*2} & 2a^* & \lambda^* \end{vmatrix} = 0 \tag{D22}$$

Equation (D22) simplifies to the following expression

$$p^{*2} + q^{*2} + 2p^*a^* = \frac{-a^*(1 + 2\lambda^*\zeta_z) + \lambda^*}{\lambda^*} \tag{D23}$$

It follows from equations (D5) and (D6) by eliminating $(1 - X)$ that

$$(p^{*2} + q^{*2})[\lambda^* - a^*(1 + 2\lambda^*\zeta_z)] - 2p^*a^*\lambda^* = 0 \tag{D24}$$

Equations (D12), (D23), and (D24) are linear in $(p^{*2} + q^{*2})$ and $2p^*$. The corresponding eliminant is

$$\begin{vmatrix} a^* & 1 & -a^* + 2\zeta_z \\ 1 & a^* & \dfrac{a^*(1 + 2\lambda^*\zeta_z) - \lambda^*}{\lambda^*} \\ \lambda^* - a^*(1 + 2\lambda^*\zeta_z) & -a^*\lambda^* & 0 \end{vmatrix} = 0 \tag{D25}$$

which simplifies to

$$(-a^* + \lambda^*)^2 = a^{*2}(\lambda^{*2} - 2\lambda^*\zeta_z) \tag{D26}$$

It follows from equation (D26) that this solution can hold only if

$$\lambda^{*2} - 2\lambda^*\zeta_z \geq 0$$

or

$$\zeta_z \leq \frac{\lambda^*}{2} \tag{D27}$$

The appropriate solution of equation (D26) is

$$-a^* + \lambda^* = a^*\sqrt{\lambda^{*2} - 2\lambda^*\zeta_z}$$

or

$$a^* = \frac{\lambda^*}{1 + \sqrt{\lambda^{*2} - 2\lambda^*\zeta_z}} \tag{D28}$$

Eliminating $p^{*2} + q^{*2}$ between equations (D12) and (D24) and substituting for a^* from equation (D28) yields the following expression for p^*

$$p^* = \frac{\lambda^*}{2(1 + 2\sqrt{\lambda^{*2} - 2\lambda^*\zeta_z} - 2\lambda^*\zeta_z)} - \zeta_z \tag{D29}$$

Equation (D4) then provides the value of X corresponding to the fastest divergence, thus,

$$X = 1 - \frac{\sqrt{\lambda^{*2} - 2\lambda^*\zeta_z} - 2\lambda^*\zeta_z}{(1 + \sqrt{\lambda^{*2} - 2\lambda^*\zeta_z})(1 + 2\sqrt{\lambda^{*2} - 2\lambda^*\zeta_z} - 2\lambda^*\zeta_z)} \tag{D30}$$

Since $X < 1$ it follows from equation (D30) that

$$\sqrt{\lambda^{*2} - 2\lambda^*\zeta_z} - 2\lambda^*\zeta_z > 0$$

or

$$\zeta_z < \frac{\sqrt{1 + 4\lambda^{*2}} - 1}{4\lambda^*} \tag{D31}$$

Since $(\sqrt{1 + 4\lambda^{*2}} - 1)/4\lambda^* < \lambda^*/2$ it follows that inequality (D31) is a more stringent limitation on permissible value of ζ_z than is inequality (D27).

The imaginary part of the complex root may be obtained from equation (D12); thus,

$$q^{*2} = -\frac{2}{a^*}(p^* + \zeta_z) + 1 - p^{*2} \tag{D32}$$

APPENDIX E

EVALUATION OF THE MAXIMUM VALUE OF $m_{d_m}^*$

For any value of X and λ^* the value of $m_{d_m}^*$ given in figure 9 satisfies equation (92) with m_d^* replaced by $m_{d_m}^*$. Thus,

$$\frac{\kappa^{*3}\lambda^* X}{1 - X} - \kappa^{*2}\{m_{d_m}^* + \lambda^{*2}[m_{d_m}^* - (1 - m_{d_m}^*)X]\}$$

$$-\kappa^*\lambda^*[m_{d_m}^*\lambda^{*2}(1 - m_{d_m}^*)(1 - X) + m_{d_m}^* - (1 - m_{d_m}^*)X] + (1 - m_{d_m}^*)\lambda^{*2}X = 0 \qquad \text{(E1)}$$

Furthermore the computer study which resulted in figure 9 shows that equation (E1) has one real negative root and a pair of equal positive roots. Therefore equation (E1) may be represented in the form

$$(\kappa^* + a)(\kappa^* - b)^2 = 0 \qquad \text{(E2)}$$

or

$$\kappa^{*3} + \kappa^{*2}(a - 2b) + \kappa^*(b^2 - 2ab) + ab^2 = 0 \qquad \text{(E3)}$$

Equating coefficients of equations (E1) and (E3) produces

$$a - 2b = -\{m_{d_m}^* + \lambda^{*2}[m_{d_m}^* - (1 - m_{d_m}^*)X]\}\frac{1 - X}{\lambda^* X} \qquad \text{(E4)}$$

$$b^2 - 2ab = -[m_{d_m}^*(1 - m_{d_m}^*)(1 - X)\lambda^{*2} + m_{d_m}^* - (1 - m_{d_m}^*)X]\frac{1 - X}{X} \qquad \text{(E5)}$$

$$ab^2 = (1 - m_{d_m}^*)(1 - X)\lambda^* \qquad \text{(E6)}$$

A necessary condition for $m_{d_m}^*$ to be a maximum with respect to variations in λ^* is $(\partial m_{d_m}^*/\partial\lambda^*) = 0$. Differentiating equations (E4), (E5), and (E6) with respect to λ^* and using this condition gives the following equations

$$\frac{\partial a}{\partial\lambda^*} - \frac{2\partial b}{\partial\lambda^*} = \frac{1 - X}{\lambda^{*2}X}\{m_{d_m}^* - \lambda^{*2}[m_{d_m}^* - (1 - m_{d_m}^*)X]\} \qquad \text{(E7)}$$

$$(b - a)\frac{\partial b}{\partial\lambda^*} - \frac{b\,\partial a}{\partial\lambda^*} = -\frac{1 - X}{X} m_{d_m}^*(1 - m_{d_m}^*)(1 - X)\lambda^* \qquad \text{(E8)}$$

$$b^2 \frac{\partial a}{\partial \lambda^*} + 2ab \frac{\partial b}{\partial \lambda^*} = (1 - m_{d_m}^*)(1 - X) \tag{E9}$$

Eliminating $\partial a/\partial \lambda^*$ and $\partial b/\partial \lambda^*$ gives

$$-\frac{1 - X}{\lambda^{*2} X} \{m_{d_m}^* - \lambda^{*2}[m_{d_m}^* - (1 - m_{d_m}^*)X]\}b^2$$

$$+ 2 \frac{(1 - X)^2}{X} m_{d_m}^*(1 - m_{d_m}^*)\lambda^* b - (1 - m_{d_m}^*)(1 - X) = 0 \tag{E10}$$

It is convenient at this stage to introduce a variable ξ defined by

$$\xi \triangleq m_{d_m}^* \frac{1 - X}{X}$$

Equations (E4), (E5), (E6), and (E10) can then be rewritten as

$$a - 2b = -\xi \frac{1 + \lambda^{*2}}{\lambda^*} + (1 - m_{d_m}^*)(1 - X)\lambda^* \tag{E11}$$

$$b^2 - 2ab = -\xi[\lambda^{*2}(1 - m_{d_m}^*)(1 - X) + 1] + (1 - m_{d_m}^*)(1 - X) \tag{E12}$$

$$ab^2 = (1 - m_{d_m}^*)(1 - X)\lambda^* \tag{E13}$$

$$\left[\xi \frac{1 - \lambda^{*2}}{\lambda^*} + (1 - m_{d_m}^*)(1 - X)\lambda^*\right]b^2 - 2\xi\lambda^{*2} b(1 - m_{d_m}^*)(1 - X)$$

$$+ (1 - m_{d_m}^*)(1 - X)\lambda^* = 0 \tag{E14}$$

Substituting ab^2 for $(1 - m_{d_m}^*)(1 - X)\lambda^*$ (eq. (E13)) in equations (E11), (E12), and (E14) gives

$$a - 2b = -\xi \frac{1 + \lambda^{*2}}{\lambda^*} + ab^2 \tag{E15}$$

$$b^2 - 2ab = -\xi(\lambda^* ab^2 + 1) + \frac{ab^2}{\lambda^*} \tag{E16}$$

$$\xi \frac{1 - \lambda^{*2}}{\lambda^*} + ab^2 - 2\xi\lambda^* ab + a = 0 \tag{E17}$$

Substituting ξ from equation (E15) into equations (E16) and (E17) gives, after some simplification,

$$\lambda^{*3}(a^2b - 2ab^2 - a^2b^3 + 2a - b)b + \lambda^{*2}(a - 2b) + \lambda^{*}(2ab - b^2) + ab^2 = 0 \qquad \text{(E18)}$$

$$\lambda^{*2}(a^2b - 2ab^2 - a^2b^3 + a - b) + (b + ab^2) = 0 \qquad \text{(E19)}$$

If a solution exists then equations (E18) and (E19) must have a common root. The dialytic eliminant of equations (E18) and (E19) is

$$\begin{vmatrix} (a^2b - 2ab^2 - a^2b^3 + 2a - b)b & a - 2b & 2ab - b^2 & ab^2 & 0 \\ 0 & (a^2b - 2ab^2 - a^2b^3 + 2a - b)b & a - 2b & 2ab - b^2 & ab^2 \\ 0 & 0 & a^2b - 2ab^2 - a^2b^3 + a - b & 0 & b + ab^2 \\ 0 & a^2b - 2ab^2 - a^2b^3 + a - b & 0 & b + ab^2 & 0 \\ a^2b - 2ab^2 - a^2b^3 + a - b & 0 & b + ab^2 & 0 & 0 \end{vmatrix} = 0 \qquad \text{(E20)}$$

It can be shown by direct substitution that equation (E20) is satisfied when

$$a = b \qquad \text{(E21)}$$

Substituting a for b in equation (E18) then yields

$$\lambda^{*} = \frac{1}{a} \qquad \text{(E22)}$$

From equation (E15) substituting for λ^* and b from equations (E22) and (E21), respectively, gives the following expression for ξ

$$\xi = m_{d_m}{}^{*} \frac{1 - X}{X} = a^2 \qquad \text{(E23)}$$

Eliminating a from equations (E23) and (E13) then gives

$$m_{d_m}{}^{*} = (m_{d_m}{}^{*})_{max} = X \qquad \text{(E24)}$$

from which it follows that

$$a = \sqrt{1 - X} \qquad \text{(E25)}$$

From equations (E22), (E24), and (E25)

$$(m_{d_m}{}^{*})_{max} = 1 - \frac{1}{\lambda^{*2}} \qquad \text{(E26)}$$

The graph of equation (E26) is shown by the dashed line in figure 9.

REFERENCES

1. Frisch, Harold P.: Thermal Bending Plus Twist of a Thin-Walled Cylinder of Open Section With Application to Gravity Gradient Booms. NASA TN D-4069, 1967.

2. Frisch, Harold P.: Coupled Thermally-Induced Transverse Plus Torsional Vibrations of a Thin-Walled Cylinder of Open Section. NASA TR R-333, 1970.

3. Yu, Yi-Yuan: Thermally Induced Vibration and Flutter of a Flexible Boom. J. Spacecraft and Rockets, vol. 6, no. 8, Aug. 1969, p. 902.

4. Beam, Richard M.: On the Phenomenon of Thermoelastic Instability (Thermal Flutter) of Booms With Open Cross Section. NASA TN D-5222, 1969.

5. Popov, E. P.: The Dynamics of Automatic Control Systems. Pergamon Press, Reading, Mass., Addison-Wesley Publishing Company, Inc., 1962, Chap. VII, Section 29.

6. Timoshenko, Stephen P.: Theory of Bending, Torsion and Buckling of Thin-Walled Members of Open Cross Section. J. Franklin Inst., vol. 239, nos. 3, 4, 5, Mar., Apr., May 1945.

7. Timoshenko, Stephen: Strength of Materials. Part 2, Advanced Theory and Problems. Second Edition-Seventh Printing, Ch. 2, Sect. 19, D. Van Nostrand Company, Inc., 1946.

TABLE 1. EXAMPLE BOOMS

Parameter	Boom A	Boom B	Boom C	Boom D
Radius of cross section, r, m		0.634×10^{-2}		
Wall thickness, h, m		0.5×10^{-4}		
Thermal conductivity, K, J/sec m °K		0.126×10^{3}		
Mass density, ρ, kg/m^3		0.75×10^{4}		
Specific heat, c, J/kg °K		4.18×10^{2}		
Coefficient of thermal expansion, e_c, m/m °K		0.187×10^{-4}		
Stephan-Boltzmann constant, σ, J/sec m^2 $°K^4$		5.71×10^{-8}		
Thermal radiation constant, J_s, J/sec m^2		1.385×10^{3}		
Emissivity, ε		0.035		
Absorptivity, α_s		0.13		
Young's modulus, E, n/m^2		1.31×10^{11}		
Second moment of area, I, m^4		0.41×10^{-10}		
Torsional stiffness, C, nm^2		0.93×10^{-4}		
Warping stiffness, C_1, nm^4		0.262×10^{-2}		
Absolute ambient temperature, T_o, °K		300		
λ, 1/sec (eq. (5))		1.0		
R_s, m (eq. (8))		600		
Mass per unit length, σ_m, kg/m		0.019		
Polar inertia per unit length, σ_I, kg m		0.76×10^{-6}		
Boom length, L, m	18.3	18.3	24.4	37.8
True tip mass, m_T, kg	0	1.61	3.76	3.63
Effective tip mass, $m_T + \Delta m_T$, kg	0.084	1.694	3.872	3.804
True rotational inertia of tip mass, I_ψ, kg m^2	0	1.605×10^{-3}	6×10^{-3}	6×10^{-3}
Effective rotational inertia of tip, $I_\psi + \Delta I_\psi$, kg m^2	0.565×10^{-5}	1.611×10^{-3}	6.008×10^{-3}	6.012×10^{-3}
$L\sqrt{C/C_1} = kL$	3.44	3.44	4.60	7.11

TABLE 1. EXAMPLE BOOMS - Concluded

Tip condition	Unrestrained	Restrained	Restrained	Restrained
$f_1(kL)$ (fig. 3)	0.49	0.41	0.52	0.665
$f_3(kL)$ (fig. 3)	0.29	0.275	0.37	0.51
A (eq. (27))	1.2691×10^3	1.2232×10^3	5.6802×10^3	6.2127×10^4
B (eq. (41))	8.8883×10^2	8.4286×10^2	4.7788×10^3	5.8777×10^4
D (eq. (29))	8.9688×10^3	7.5044×10^3	2.2561×10^4	1.0725×10^5
$(1/\sqrt{10})(A/D)$ (eq. (33))	0.045	0.0515	0.0796	0.184
Radius of gyration of equivalent tip mass, ρ_ψ, m	0.00632	0.0308	0.0402	0.396
$\sqrt{m_T(A - B)}$ and λ^*	5.655	25.383	58.217	111.887
X	0.700	0.689	0.8413	0.946
p^* (fig. 6)	0.142	0.042	0.048	0.075
Time to double amplitude (no damping), min	0.46	6.98	14.02	17.20

NASA-Langley, 1970 —— 32 A-3284

NATIONAL AERONAUTICS AND SPACE ADMINISTRATION
WASHINGTON, D. C. 20546

OFFICIAL BUSINESS

FIRST CLASS MAIL

POSTAGE AND FEES PAID
NATIONAL AERONAUTICS AND
SPACE ADMINISTRATION

POSTMASTER: If Undeliverable (Section 158 Postal Manual) Do Not Return

"The aeronautical and space activities of the United States shall be conducted so as to contribute . . . to the expansion of human knowledge of phenomena in the atmosphere and space. The Administration shall provide for the widest practicable and appropriate dissemination of information concerning its activities and the results thereof."

—NATIONAL AERONAUTICS AND SPACE ACT OF 1958

NASA SCIENTIFIC AND TECHNICAL PUBLICATIONS

TECHNICAL REPORTS: Scientific and technical information considered important, complete, and a lasting contribution to existing knowledge.

TECHNICAL NOTES: Information less broad in scope but nevertheless of importance as a contribution to existing knowledge.

TECHNICAL MEMORANDUMS: Information receiving limited distribution because of preliminary data, security classification, or other reasons.

CONTRACTOR REPORTS: Scientific and technical information generated under a NASA contract or grant and considered an important contribution to existing knowledge.

TECHNICAL TRANSLATIONS: Information published in a foreign language considered to merit NASA distribution in English.

SPECIAL PUBLICATIONS: Information derived from or of value to NASA activities. Publications include conference proceedings, monographs, data compilations, handbooks, sourcebooks, and special bibliographies.

TECHNOLOGY UTILIZATION PUBLICATIONS: Information on technology used by NASA that may be of particular interest in commercial and other non-aerospace applications. Publications include Tech Briefs, Technology Utilization Reports and Notes, and Technology Surveys.

Details on the availability of these publications may be obtained from:

SCIENTIFIC AND TECHNICAL INFORMATION DIVISION

NATIONAL AERONAUTICS AND SPACE ADMINISTRATION

Washington, D.C. 20546